Velocity redistribution of excited atoms by radiative excitation transfer. II. Theory of radiation trapping in collimated beams

N. N. Bezuglov
St. Petersburg State University, Fock Institute of Physics, Petrodvorets, Ulianovskaya ul.1, 198904 St. Petersburg, Russia

A. Ekers, O. Kaufmann, and K. Bergmann
University of Kaiserslautern, Department of Physics, Erwin-Schrödinger-Str., D-67663 Kaiserslautern, Germany

F. Fuso and M. Allegrini
INFM, Dipartimento di Fisica Enrico Fermi, Università di Pisa, Via F. Buonarroti 2, I-56127 Pisa, Italy

(Received 21 March 2003; accepted 11 July 2003)

We have developed a theory of resonance radiation imprisonment in collimated atomic beams. Treating the integral master equation describing imprisonment as a generalized wave (Schrödinger) equation and using the geometrical quantization technique for its solution, we obtained analytical representations for the effective radiative lifetime, mean scattering number, and trapping factors. We apply this theory to explain the recent observation of a dramatic velocity redistribution of excited atoms by radiative excitation transfer after the photofragmentation of Na_2. In this process, the fast Na$(3p)$ photofragments transfer their excitation energy efficiently via radiation to the abundant Na$(3s)$ atoms from the primary particle beam. The influence of the hyperfine splitting of the ground state of Na atoms on this process is discussed. The ratio of the number of Na$(3p)$ atoms produced by the radiative excitation transfer to the number of Na$(3p)$ photofragments was found to be 0.13 and 0.19 for photodissociation of Na_2 molecules in the vibrational levels $v''=17$ and $v''=23$, respectively. This is in good agreement with the corresponding experimental values of 0.16 and 0.22. © *2003 American Institute of Physics.* [DOI: 10.1063/1.1605378]

I. INTRODUCTION

Trapping of atomic resonance radiation in vapor (called also radiation imprisonment) was first described by Milne,[1] Holstein,[2] and Biberman[3] in the first half of the last century. If an excited atom is surrounded by other atoms of the same species in the ground state at high enough densities, the resonance radiation will be absorbed and reemitted many times before it escapes from the volume occupied by the atoms. The successive reabsorption and reemission of photons decrease the effective radiative decay rate Γ_{eff} of the ensemble of atoms in the sample compared to the spontaneous decay rate Γ_{nat}:

$$\Gamma_{\text{eff}}=g\Gamma_{\text{nat}}, \tag{1}$$

where g is a dimensionless parameter, the escape factor, which can be regarded as the reciprocal of the number of emission and absorption events before the escape. The escape factor g depends on a number of experimental conditions, like the number density and velocity distribution of absorbing atoms, the spectral line shapes, and the geometry of the region in which the atoms are confined. Although the radiation trapping has been studied for about 80 years, the complexity of this process has not allowed an adequate description except for a limited number of idealized geometries, like slabs, cylinders, or spheres[1–7] assuming a homogeneous angular distribution of atom velocities.

At first glance it may seem that the density in atomic beams is too low to cause radiation trapping. However, in this work and the preceding one we show that this is not the case. In atomic beams, the quantitative estimates of the radiation trapping are complicated by the inhomogeneity in the velocity distribution (and, hence, the spectral line shapes) of atoms in the beam. This inhomogeneity causes difficulties in the mathematical description of the phenomenon.[8,9] For this reason radiation trapping under atomic beam conditions is poorly presented in the literature.

An important implication of radiation trapping is the increase of the effective lifetime τ_{eff} of an ensemble of excited atoms compared to the spontaneous lifetime τ_{nat} of a single isolated atom. However, this is not the only consequence to be considered. In the context of photodissociation processes an earlier study[10] considered radiation trapping in a vapor cell as a process affecting the measurement of absolute intensity of the fluorescence emitted by excited photofragments. An experiment on molecule–atom collisional energy transfer[11] has qualitatively shown how the radiation trapping changes the spatial distribution of excited atoms in a resonance state in an effusive molecular beam. Yet another study[12] has demonstrated that radiation trapping plays a dominant role in the thermalization of velocity-selected excited atoms in thermal vapors. Probably the most spectacular manifestation of radiation trapping is the recent experimental observation of a dramatic velocity redistribution of excited atoms after a photodissociation process, which is described in the preceding publication[13] (hereafter referred to as Paper I). In this study Na_2 molecules in a supersonic beam were selectively prepared in single excited rovibronic levels of the electronic ground state $X\,^1\Sigma_g^+$ and photodissociated by ab-

sorption of a photon from a fixed frequency laser via the $B\,^1\Pi_u$ state:

$$\mathrm{Na}_2(X\,^1\Sigma_g^+, v''J'') + h\nu \rightarrow \mathrm{Na}_2^*(B\,^1\Pi_u) \rightarrow \mathrm{Na}^*(3p_{3/2}) + \mathrm{Na}(3s_{1/2}) + \Delta E_{\mathrm{kin}}. \tag{2}$$

The velocity distributions of the Na($3p$) photofragments were measured using an ion imaging technique. This photodissociation process produces Na($3p$) and Na($3s$) fragments with well-defined kinetic energies depending on the internal excitation of the Na_2 molecule prior to dissociation and the energy of the absorbed photon. The experiments showed, however, that besides the expected fast Na($3p$) atoms a relatively large fraction of ''slow'' Na($3p$) atoms is also produced. Here ''slow'' means that the atoms maintain their initial velocity in the beam, but do not acquire additional kinetic energy. In particular, their velocity component perpendicular to the molecular beam axis remains small. The ratio of ''slow'' to ''fast'' Na($3p$) atoms was measured to be 0.16 and 0.22 for dissociation of Na_2 in vibrational levels $v''=17$ and $v''=23$, respectively. This observation was interpreted as a consequence of radiative excitation transfer from the ''fast'' Na($3p$) photofragments to Na($3s$) atoms in the primary particle beam:

$$\text{fast Na}^*(3p_{3/2}) + \text{slow Na}(3s_{1/2}) \rightarrow \text{fast Na}(3s_{1/2}) + \text{slow Na}^*(3p_{3/2}). \tag{3}$$

We shall hereafter refer to this process as *radiative excitation transfer* (RADEXT).

The scope of the present paper is twofold. First, we provide a detailed analytical description of radiation imprisonment (RI) in collimated atomic beams. Second, we demonstrate how this phenomenon implies remarkable changes in the apparent translation energy distribution of excited species after a unimolecular fragmentation process. Analysis of RI under the particular conditions of the experiment described in Paper I shows that the observed velocity redistribution of excited atoms can indeed be quantitatively described.

The paper is organized as follows: In Sec. II, the spectral absorption coefficient for a highly collimated atomic beam is derived and the consequences of the photon emission–absorption sequence are discussed. It is shown that radiation trapping does not change the velocities of slow excited atoms in the primary beam. This result allows us to separate the spatial and velocity variables in the master equation describing the dynamics of the excited states. In Sec. III, the escape factors are evaluated under steady-state conditions. The equation for the mean number of scattering events of a photon initially emitted at an arbitrary point in space is derived using different methods which allow an estimation of the accuracy of the calculations. The expressions obtained for the escape factors allow us to find the total number of excited atoms for an arbitrary spatial distribution of the excitation sources. Section IV analyzes the Holstein trapping factors g_j. They are connected to the effective lifetimes of modes (eigenfunctions) of the imprisonment equation. The spectral problem, which includes the determination of the overall spectrum of eigenmodes and the radiative decay constants, is solved using the *geometrical quantization technique* (GQT) first described in Refs. 4 and 14. This approximation is a rather universal and yet accurate analytical method which can be used for the treatment of a wide class of integro-differential transport equations. We exploit then GQT (in Sec. IV D) to reduce the RI master equation to an equation of Fokker–Planck (FP) type. Section V describes the excitation source function formed due to the emission of photons by fast Na($3p$) photofragments. Section VI is devoted to the RADEXT processes. We apply the theory to the experiment described in Paper I and discuss the influence of hyperfine splitting of Na energy levels on RADEXT. Analytical expressions for the ratio of the number of slow Na($3p$) atoms produced in the RADEXT process (3) to the number of fast source Na($3p$) atoms which are produced in the photodissociation are obtained. The results are compared to the experimental data of Paper I. In Appendix A, the details of the Fourier transformation of the RI master equation necessary for the calculations by GQT are given. In Appendix B, the derivation of equations describing the relation between the total number of slow Na($3p$) atoms formed due to RADEXT and the number of excited photofragments is given. This derivation provides also a justification of some of the assumptions which are made in the present paper. In Appendix C, the effect of hyperfine splitting of Na ground state on radiation imprisonment is considered. For readers mainly interested in ready-to-use analytical formulas for calculation of trapping factors, Secs. II, III, and VI are most relevant.

II. FORMULATION OF THE PROBLEM

The extent of radiation imprisonment is determined by the absorption coefficient of the medium κ_ν. The latter depends on the velocity distribution $f(\vec{v})$ of absorbing atoms. Suppose the medium is a collimated supersonic beam. For illustration we choose the parameters of a Na/Na_2 beam used for the experiments in Paper I. The flow velocity of atoms in the beam $v_f = 1340$ m/s, with a full 1/e widths of the velocity distributions of ground-state atoms and molecules along the beam axis of $\Delta v_{\mathrm{at}} = 300$ m/s and $\Delta v_{\mathrm{mol}} = 260$ m/s, respectively. In the direction perpendicular to the beam axis the atoms are collimated to a divergence of 0.8°, which corresponds to a velocity spread of 9 m/s. Such small transverse velocity spread allows us to assume for further mathematical analysis that the beam is ideally collimated: i.e., we neglect the deviation of the velocity vectors of atoms from the particle beam axis $\vec{e}_y$. The normalized velocity distributions of Na($3s$) atoms and Na_2 molecules in the beam thus become

$$f_i(\vec{v}) = \delta(v_x)\,\delta(v_z)\,f_i(v_y),$$
$$f_i(v) = \frac{1}{\sqrt{\pi}\Delta v_i}\exp\left(-\frac{v^2}{\Delta v_i^2}\right), \tag{4}$$
$$\int_{-\infty}^{\infty} dv\; f_i(v) = 1,$$

where $i=\{\mathrm{at},\mathrm{mol}\}$ stays for atoms or molecules and the symbol δ denotes the Dirac function, while velocity v_y is measured relative to the mean flow velocity v_f of the beam. Note that only this relative velocity is of importance for the fol-

lowing theoretical treatment; therefore, the flow velocity is hereafter disregarded. Furthermore, we assume that the spectral absorption and emission profiles κ_ν and φ_ν are determined by the Doppler profile, which is justified since the characteristic Doppler frequency shift $\Delta\nu_D \sim \Delta v/\lambda$ is much larger than the natural linewidth $\Gamma_{\rm nat}$. The absorption coefficient for a photon of frequency ν moving in the direction $\vec{n}$ is then given by the relation[15]

$$\kappa_\nu = \overline{\sigma}^{(r)} \Gamma_{\rm nat} N_0 \frac{c}{\nu_0} \int d^3v\, f_{\rm at}(\vec{v})\, \delta\left(\vec{n}\cdot\vec{v} - \frac{\nu-\nu_0}{\nu_0}c\right),$$
$$\overline{\sigma}^{(r)} = \frac{\lambda^2}{8\pi}\frac{\overline{g}_{3/2}}{\overline{g}_{1/2}}, \tag{5}$$

where c is the speed of light, ν_0 and λ are the frequency and wavelength of resonance photons in the line center, $\overline{g}_{1/2}=2$ and $\overline{g}_{3/2}=4$ are the statistical weights of the lower $3s_{1/2}$ and upper $3p_{3/2}$ levels, respectively, and $N_0 = 2\times 10^{11}\,{\rm cm}^{-3}$ gives the density of the absorbing Na($3s_{1/2}$) atoms. Using the distribution (4), Eq. (5) reduces to

$$\kappa_\nu = \frac{\kappa_0}{|\cos\theta|}\sqrt{\pi}\Delta v_{\rm at}\, f_{\rm at}\left(\frac{v_\nu}{|\cos\theta|}\right), \quad v_\nu = \frac{\nu-\nu_0}{\nu_0}c,$$
$$\kappa_0 \equiv \frac{\lambda^3}{8\pi^{3/2}}\frac{\overline{g}_{3/2}}{\overline{g}_{1/2}}\frac{\Gamma_{\rm nat}}{\Delta v_{at}}N_0. \tag{6}$$

Here θ is the angle between the direction $\vec{n}$ of the photon propagation and the beam axis y (see Fig. 1) and $\kappa_0 = 3.7\,{\rm cm}^{-1}$ is the Doppler absorption coefficient at the line center at $\lambda = 589.16$ nm (the conditions of Paper I). From Eq. (6) it is clear that the absorption at the center of line is large in directions perpendicular to the particle beam axis because the width $\Delta\nu_D \sim |\cos\theta|$ of the Doppler profile decreases when the angle θ increases from 0° to 90°. This effect outweighs the relatively small opacity $\kappa_0 R = 0.37$ of the beam with radius $R = 0.1$ cm, so that radiation imprisonment becomes noticeable even under the supersonic beam conditions.

The generalized master equation describing the evolution of the density $n^*_{\rm slow}(\vec{r},v_y,t)$ of excited resonance atoms is given by Holstein[2] and Biberman:[3,16]

$$\frac{\partial}{\partial t}n^*_{\rm slow}(\vec{r},v_y,t) = -(\Gamma_{\rm nat}+W)n^*_{\rm slow}(\vec{r},v_y,t) + S^*(\vec{r},v_y) + \Gamma_{\rm nat}\hat{G}n^*_{\rm slow}(\vec{r},v_y,t). \tag{7}$$

The excited atoms decay due to spontaneous emission (rate $\Gamma_{\rm nat}$) and collisional quenching (rate W). In what follows we neglect the quenching rate unless indicated otherwise. The density n^* is a function of both the location of atoms and their velocity. For collimated beams the analysis of the velocity distribution simplifies considerably. As will be shown below [see the discussion after Eq. (45)], the RADEXT from fast Na($3p_{3/2}$) photofragments creates the initial ensemble of slow Na($3p_{3/2}$) atoms determining the excitation source function S^*. The velocity distribution of the source function, $\tilde{f}(v_y)$, appears to be very close to the velocity distribution of ground-state atoms in the beam:

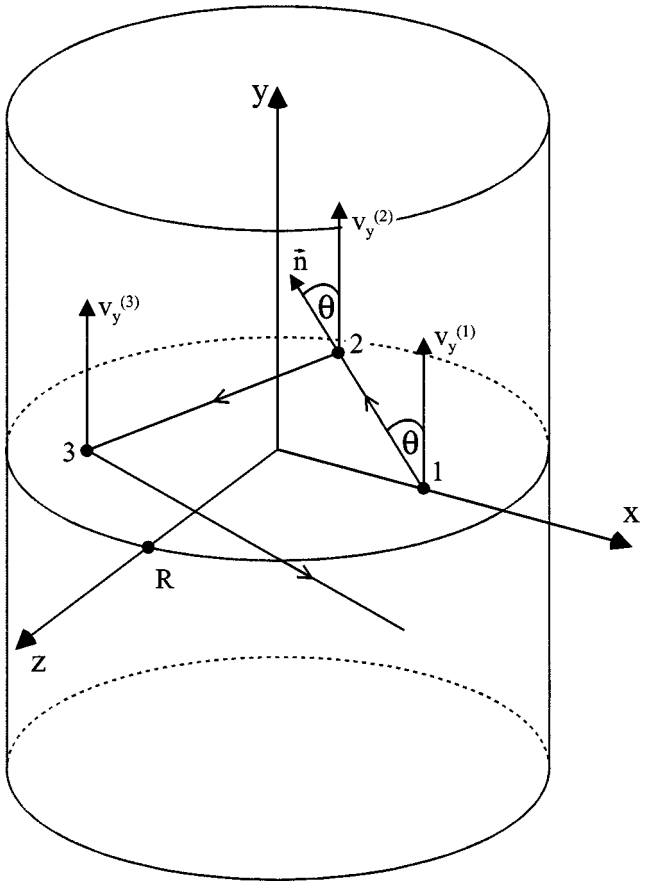

FIG. 1. Illustration of the imprisonment of resonant radiation within an ideally collimated atomic beam. The Doppler effect implies that the photon emitted in the direction $\vec{n}$ by atom (1) moving with the velocity $\vec{v}_y^{(1)}$ along the particle beam axis can be absorbed only by such atom (2) whose velocity $\vec{v}_y^{(2)}$ has the same projection on the direction of $\vec{n}$ as the velocity of the emitting atom (1): $\vec{v}_y^{(1)}\vec{n} = \vec{v}_y^{(2)}\vec{n}$. This condition is valid for each pair of emission-absorption events.

$$S^*(\vec{r},v_y) = S^*(\vec{r})\tilde{f}(v_y), \quad \tilde{f}(v_y) \simeq f_{\rm at}(v_y). \tag{8}$$

The source function $S^*(\vec{r}) = \int dv_y S^*(\vec{r},v_y)$ describes the external excitation rate [${\rm cm}^{-3}\,{\rm s}^{-1}$]. The factorization (8) is valid for most of the practical situations, like excitation due to laser irradiation or collisions, but the velocity distribution $\tilde{f}(v_y)$ depends on the specific parameters of the experiment.

The last term in Eq. (7), $\hat{G}n^*_{\rm slow}$, describes the imprisonment of radiation within the volume Ω_b occupied by the absorbing atoms. Without imprisonment, Eq. (7) reduces to a conventional rate equation where the excited atoms decay at a spontaneous decay rate $\Gamma_{\rm nat}$. When $\hat{G}n^*_{\rm slow}$ becomes nonnegligible, RI leads to a smaller effective decay rate $\Gamma_{\rm eff}$ [see Eq. (1)]. We now seek an explicit representation of the imprisonment term $\hat{G}n^*_{\rm slow}$. Suppose a slow Na($3p_{3/2}$) atom at point 1 (see Fig. 1) moves with the velocity $v_y^{(1)}$ and emits a photon in the direction $\vec{n}$. Due to the Doppler shift with respect to an atom absorbing the photon at point 2, we require the conservation of the velocity projection on $\vec{n}$: $(v_y^{(1)}\vec{e}_y)\vec{n} = (v_y^{(2)}\vec{e}_y)\vec{n}$, i.e., $v_y^{(1)} = v_y^{(2)}$. In other words, the photon reabsorption in the system of slow Na($3p_{3/2}$) atoms does not change the velocity v_y of the atoms involved. The frequency of the photons seen by the atoms is $\nu = \nu_0$

$+\nu_0 c^{-1}(v_y\vec{e}_y)\vec{n}=\nu_0+\cos\theta v_y\lambda^{-1}$ and is thus strongly dependent on the direction of photon propagation. Due to the conservation of v_y during successive absorption processes (see Fig. 1), the formation of slow excited atoms can be considered separately for each subensemble Ξ_v with fixed velocity $v=v_y$. Taking into account the factorization (8), we rewrite Eq. (7) in the form

$$\frac{\partial}{\partial t}n_v^*(\vec{r},t)=-\Gamma_{\rm nat}n_v^*(\vec{r},t)+\Gamma_{\rm nat}\int_{\Omega_b}d^3r'\,G_v(\vec{r},\vec{r}')\times n_v^*(\vec{r}',t)+S^*(\vec{r}),$$
$$n^*_{\rm slow}(\vec{r},v_y,t)=n^*_{v_y}(\vec{r},t)\tilde{f}(v_y), \tag{9}$$

$$G_v(\vec{r},\vec{r}')=\frac{1}{4\pi|\vec{r}-\vec{r}'|^2}\frac{\zeta_v}{\cos\theta}\exp\left(-\frac{\zeta_v}{\cos\theta}|\vec{r}-\vec{r}'|\right),$$
$$\zeta_v=\kappa_0\exp\left(-\frac{v_y^2}{\Delta v_{\rm at}^2}\right). \tag{10}$$

The kernel G_v of the integral operator $\hat{G}n^*_{\rm slow}$ gives the probability that photon emitted at point $\vec{r}'$ will be absorbed at point $\vec{r}$. The effective absorption coefficient $\zeta_v/\cos\theta$ for the subensemble Ξ_v is derived from Eq. (6), while the angle θ is measured between the vector $\vec{r}-\vec{r}'$ and the beam axis y. Note that we deal with population of excited states and are not interested in polarization[17] and alignment[18] phenomena. As was shown in Refs. 18 and 19, the polarization properties of the radiation do not noticeably influence the excited-state density in the vapor provided no special efforts are undertaken for preparing strong atom alignment. Mathematically, ignoring polarization effects corresponds to angular isotropic emission of photons and results in the factor $1/4\pi$ entering expression (10) for the kernel G_v.

III. ESCAPE FACTORS UNDER STEADY-STATE CONDITIONS

When steady-state conditions apply (as in the case of the experiment described in Paper I), the RI master Eq. (9) simplifies significantly:

$$n_v^*(\vec{r})-\int_{\Omega_b}d^3r'\,G_v(\vec{r},\vec{r}')n_v^*(\vec{r}')=\frac{S^*(\vec{r})}{\Gamma_{\rm nat}}. \tag{11}$$

It will prove beneficial to write the solution of Eq. (11) in an operator notation, $n_v^*(\vec{r})=\Gamma_{\rm nat}^{-1}(\hat{I}-\hat{G}_v)^{-1}S^*(\vec{r})$, and consider the total number N_v^* of excited atoms in the ensemble Ξ_v:

$$N_v^*\equiv\int_{\Omega_b}d^3r n_v^*(\vec{r})=\frac{1}{\Gamma_{\rm nat}}\int_{\Omega_b}d^3r(\hat{I}-\hat{G}_v)^{-1}S^*(\vec{r})=\frac{1}{\Gamma_{\rm nat}}\langle 1|(\hat{I}-\hat{G}_v)^{-1}|S^*\rangle. \tag{12}$$

Here, the scalar product of two functions, $\langle g|h\rangle=\int d^3r\,g(\vec{r})h(\vec{r})$, is introduced. The symbol $|1\rangle$ denotes a function g identical to unity, i.e., $g=|1\rangle\Leftrightarrow g(\vec{r})\equiv 1$. Since the operator $\hat{G}_v$ is Hermitian (symmetrical with respect to its arguments), Eq. (12) has an equivalent representation

$$N_v^*=\frac{1}{\Gamma_{\rm nat}}\langle S^*|(\hat{I}-\hat{G}_v)^{-1}|1\rangle=\frac{1}{\Gamma_{\rm nat}}\int_{\Omega_b}d^3r\,S^*(\vec{r})\overline{N}_v(\vec{r}),$$
$$\overline{N}_v(\vec{r})\equiv(\hat{I}-\hat{G}_v)^{-1}|1\rangle, \tag{13}$$

where $\overline{N}_v$ can be interpreted as the mean number of scattering events experienced by a photon initially emitted at the point $\vec{r}$ (Ref. 15). Indeed, if we restrict the excitation (with the total intensity $S_0^*\,[{\rm s}^{-1}]$ to a single point $\vec{r}=\vec{r}_0$, the source function becomes $S^*(\vec{r})=S_0^*\delta^{(3)}(\vec{r}-\vec{r}_0)$, where $\delta^{(3)}$ is the three-dimensional Dirac delta function. The total number of excited atoms, $N_v^*=S_0^*\Gamma_{\rm nat}^{-1}\overline{N}_v(\vec{r}_0)$, is then determined by the effective radiative lifetime: $N_v^*=S_0^*\tau_{\rm eff}$. The amount by which $\tau_{\rm eff}=\tau_{\rm nat}\overline{N}_v(\vec{r}_0)$ exceeds the natural lifetime $\tau_{\rm nat}$ in a transparent medium is thus determined by the number $\overline{N}_v(\vec{r}_0)$ of photon captures. Calculating the total number of excited atoms by integration over the beam volume according to Eq. (13) is simpler than by solving the integral Eq. (11).

Equation (13) implies that $\overline{N}_v$ satisfies a relation $(\hat{I}-\hat{G}_v)\overline{N}_v(\vec{r})=1$, i.e.,

$$\overline{N}_v(\vec{r})-\int_{\Omega_b}d^3r'\,G_v(\vec{r},\vec{r}')\overline{N}_v(\vec{r}')=1. \tag{14}$$

Because of the cylindrical symmetry of the kernel G_v, the mean scattering number $\overline{N}_v(\vec{r})$ depends only on the distance r_b of point $\vec{r}$ from the axis of the particle beam, so that $\overline{N}_v(\vec{r})\equiv\overline{N}_v(r_b)$. Let us determine the mean scattering number $N_v(r_b)$. We shall use for this purpose two independent approaches which should allow the assessment of the accuracy of estimates.

A. Mean number of scattering events $\overline{N}_v$ at large opacities: Fokker–Planck technique

The kernel G_v, Eq. (10), is an exponential function of space coordinates which implies a finite mean free path value for a photon imprisoned in the system Ξ_v. Therefore it is justified to use the Milne approach[1] for transforming the integral Eq. (14) into a differential equation of Fokker–Planck type.[20,17] For a cylindrically symmetric medium with large opacity $\kappa_0 R\gg 1$, Eq. (14) can be approximated by the following diffusion problem (we refer the interested reader to Refs. 20 and 17):

$$(\hat{I}-\hat{G}_v)\overline{N}_v(r_b)=1,$$
$$(\hat{I}-\hat{G}_v)\overline{N}_v(r_b)=-\frac{1}{15\zeta_v^2}\frac{1}{r_b}\frac{d}{dr_b}r_b\frac{d}{dr_b}. \tag{15}$$

The photons are not reflected from the boundary of the sample considered, but escape from the volume. Therefore the diffusion Eq. (15) must be supplemented by a boundary condition

$$-\frac{d}{dr_b}\overline{N}_v(r_b)=\sqrt{15}\zeta_v\overline{N}_v(r_b)\big|_{r_b=R}. \tag{16}$$

The derivation of the expressions given by Eqs. (15) and (16) is relegated to Sec. IV where a general representation of the RI equation is obtained. At large opacities, Eqs. (15) and (16) have an exact analytical solution $\bar{N}_v^{(\mathrm{large})}(r_b)=0.5\sqrt{15}\zeta_v R+3.75(\zeta_v R)^2(1-r_b^2R^{-2})$. The method for extrapolating $\bar{N}_v^{(\mathrm{large})}$ to the region of small opacities is described in Sec. IV. In essence, the procedure consists of two steps. In a transparent medium ($\kappa_0 R\to 0$) a photon is emitted only once without reabsorption. Therefore the condition $\bar{N}_v(r_b)\equiv 1$ needs to be fulfilled. That condition can easily be satisfied by setting $\bar{N}_v=1+\bar{N}_v^{(\mathrm{large})}$. However, the discussion in Sec. IV D. shows that such extrapolation alone does not ensure a satisfactory accuracy. We follow therefore a generally accepted procedure in the treatment of RI which reduces the radiation transfer equations to a form equivalent to the one describing a Brownian-type motion of photons in the absorbing medium.[17] In this method a correction is obtained (see Sec. IV D) by rescaling the opacity $\zeta_v R$ with $\zeta_v\tilde{R}$:

$$\bar{N}_v(r_b)=1+\frac{\sqrt{15}}{2}\zeta_v\tilde{R}+\frac{15}{4}(\zeta_v\tilde{R})^2\left(1-\frac{r_b^2}{\tilde{R}^2}\right),$$
$$\tilde{R}=R\left(1+\frac{1}{0.2+5.47\zeta_v R+0.169(\zeta_v R)^2}\right). \tag{17}$$

The accuracy of this extrapolation can be examined by comparison with results of an independent approach suggested in Ref. 3, which is valid for small opacities.

B. Mean number of scattering events $\bar{N}_v$ at low opacities: Biberman method

We now solve Eq. (14) using the Biberman method.[3,16,21] At small opacities $\kappa_0 R<0.5$, the mean number of scattering events, $\bar{N}_v(r_b)$, is a slowly varying function of r_b [see Eq. (17)]. One can therefore replace $N_v(\vec{r}\,')$ in Eq. (14) by its value at $\vec{r}\,'=\vec{r}$:

$$\bar{N}_v(\vec{r})\left[1-\int_{\Omega_b}d^3r'\,G_v(\vec{r},\vec{r}\,')\right]=1. \tag{18}$$

For determination of the accuracy of Eq. (17) it is sufficient to consider the value of $\bar{N}_v$ at $r_b=0$, i.e., when $\vec{r}$ lies on the beam axis. After introducing spherical coordinates (r',φ,θ), as depicted in Fig. 2, the integration over the radial coordinate r' and azimuthal angle φ yields immediately

$$\bar{N}_v(r_b=0)M_{\mathrm{eff}}=1,$$
$$M_{\mathrm{eff}}=\frac{1}{2}\int_0^{\pi}d\theta\sin\theta\exp\left(-\zeta_v R\frac{1}{\sin\theta\cos\theta}\right). \tag{19}$$

Here M_{eff} is the so called Biberman escape factor, which gives the probability that a photon emitted at the beam axis escapes from the beam volume Ω_b without absorption. Figure 3(a) compares M_{eff}^{-1} with the number of scattering events, $\bar{N}_v(r_b=0)$, determined from Eq. (17). Under the conditions of the experiment discussed Paper I ($\zeta_v R\leqslant\kappa_0 R=0.37$) the deviation of $\bar{N}_v(r_b=0)$ from M_{eff}^{-1} does not exceed 10%. In fact, the Biberman escape factor (19) can be expanded in a series of the opacity parameter $\zeta_v R$ (Ref. 22):

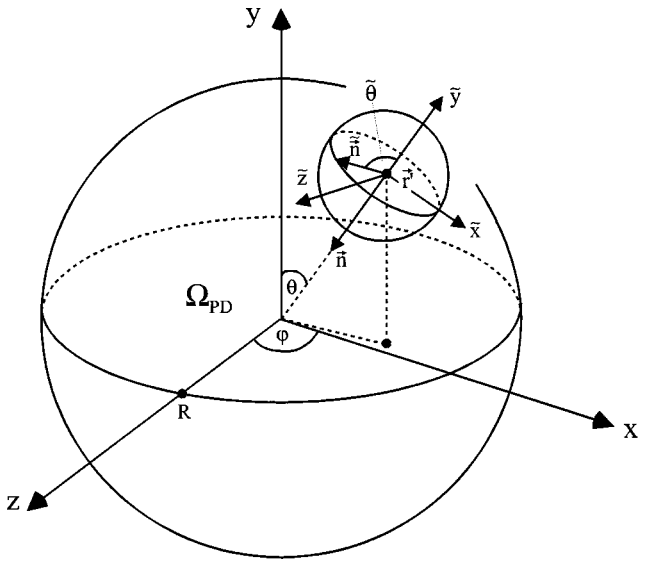

FIG. 2. Spherical coordinate systems used to derive the source function $S^*(\vec{r}=0)$ due to radiative excitation transfer from fast Na($3p_{3/2}$) atoms to slow Na($3s_{1/2}$) atoms. The photon is emitted at point $\vec{r}\,'$ by a fast photofragment and absorbed by a slow ground-state atom at the center ($\vec{r}=0$) of the photodissociation zone Ω_{PD}. Using two steps of Euler transformation, the coordinate system $\{x,y,z\}$ related to the absorbing slow atoms at $\vec{r}=0$ is replaced by a coordinate system $\{\tilde{x},\tilde{y},\tilde{z}\}$ related to a photofragment at $\vec{r}=\vec{r}\,'$ emitting a photon in the direction $\vec{n}=-\vec{e}_{\tilde{y}}$.

$$M_{\mathrm{eff}}=1+\zeta_v R\left[\ln\left(\frac{\zeta_v R}{2}\right)-1+\mathbf{C}\right]-\frac{(\zeta_v R)^2}{2}\left[\ln\left(\frac{\zeta_v R}{2}\right)-0.5+\mathbf{C}\right]+\cdots, \tag{20}$$

where $\mathbf{C}=0.57722...$ is the Euler constant.[23] This expansion is accurate within the range of validity ($\kappa_0 R<0.5$) of the Biberman approach [see Fig. 3(a)].

IV. EFFECTIVE RADIATIVE LIFETIMES UNDER TIME-DEPENDENT CONDITIONS

In order to justify the use of the relations given by the Eqs. (15), (16), and (17), we exploit another interpretation of the mean scattering number $\bar{N}_v$ given in Refs. 9, 24, and 25. We demonstrate that $\bar{N}_v(r_b)$ is closely related to the effective decay rate of an ensemble of excited atoms. Specifically, we are interested in the survival of the initial distribution $n_v^*(\vec{r},t=0)$ of excited atoms after the termination of the excitation at $t=0$, which is implemented by setting $[S^*(\vec{r})\equiv 0]$ for $t\geqslant 0$ [see Eq. (9)]. For convenience we substitute $n_v^*(\vec{r},t=0)$ by a distribution $\rho(\vec{r},t=0)=|\rho_0\rangle$ normalized to unity: $\int_{\Omega_b}d^3r\,\rho(\vec{r},t=0)=1$.

A. Time-dependent interpretation of $\bar{N}_v(r_b)$

We express the solution of the master Eq. (9), describing the time evolution of $\rho(\vec{r},t)=n_v^*(\vec{r},t)$, in terms of a Green function: $\rho(\vec{r},t)=\exp[-t\Gamma_{\mathrm{nat}}(\hat{I}-\hat{G}_v)]|\rho_0\rangle$. The probability $P(t)$ of finding an excited atom in the atomic beam volume at the moment t is then given by

$$P(t)=\int_{\Omega_b} d^3r\,\rho(\vec{r},t)=\langle 1|\exp[-t\Gamma_{\rm nat}(\hat{I}-\hat{G}_v)]|\rho_0\rangle, \tag{21}$$

where $P(t=0)=1$ thanks to the above normalization of $|\rho_0\rangle$. Following Ref. 26, we shall characterize the decay process by a mean lifetime $\tau_{\rm eff}(\rho_0)$. The probability that the excited state will decay within the time interval dt is $-dP$, where the minus sign accounts for the loss of excitation in the volume Ω_b. Therefore,

$$\begin{aligned}\tau_{\rm eff}(\rho_0)&\equiv\int_0^\infty -dP\,t\\&=\int_0^\infty dt\,P\\&=\int_0^\infty dt\langle 1|\exp[-t\Gamma_{\rm nat}(\hat{I}-\hat{G}_v)]|\rho_0\rangle\\&=\Gamma_{\rm nat}^{-1}\langle 1|(\hat{I}-\hat{G})^{-1}|\rho_0\rangle.\end{aligned}$$

Since the RI operator $\hat{G}_v$ is self-conjugated, the position of the functions $|\rho_0\rangle$ and $|1\rangle$ can be interchanged. Together with Eq. (13) we therefore obtain

$$\tau_{\rm eff}(\rho_0)=\langle\rho_0|(\hat{I}-\hat{G})^{-1}|1\rangle=\tau_{\rm nat}\int_{\Omega_b} d^3r\,\overline{N}_v(\vec{r})\rho_0(\vec{r}). \tag{22}$$

Suppose the excitation was initially located at the point $\vec{r}_0$: $\rho_0(\vec{r})=\delta^{(3)}(\vec{r}-\vec{r}_0)$. The value of $\tau_{\rm nat}\overline{N}_v(\vec{r}_0)$ has then an obvious meaning. It is the average lifetime of excitation that was initially localized at the point $\vec{r}_0$. In the more general situation of arbitrary initial spatial distribution of excited atoms the effective lifetime is found by integration over the beam volume. This explains the relation of the mean scattering number $\overline{N}_v$ with the time-dependent radiation imprisonment problems, even though the functional form of $\overline{N}_v$ is determined by the steady-state Eq. (14).

B. Holstein trapping factors and formulation of the spectral problem

Initially, Holstein introduced the escape factor g as a dimensionless parameter characterizing the decrease of the radiative decay rate of the ensemble of atoms due to radiation trapping.[2] However, in later studies it became generally accepted to use the parameters g_j to characterize the increase of the lifetime.[17] One therefore needs to distinguish the escape factor g defined by Eq. (1) from the trapping factors g_j used below.

The solution of Eq. (9) (without the source function S^*) can be expanded in the Fourier series of exponentially decaying eigenmodes $n_v^{(j)}(\vec{r},t)=\psi_j(\vec{r})\exp(-\lambda_j t)$ (Refs. 2 and 17). The eigenfunctions are found by substituting, in Eq. (9), $\partial/(\partial t)\to-\lambda_j$, where λ_j are the effective radiative decay constants (eigenvalues) of the eigenmodes. Thus, Eq. (9) reduces to the following spectral problem:

$$\begin{aligned}\lambda_j\psi_j(\vec{r})&=\Gamma_{\rm nat}(\hat{I}-\hat{G}_v)\psi_j(\vec{r})+W_\Omega\psi_j(\vec{r}),\\ \lambda_j^{-1}&=\tau_j\equiv\tau_{\rm nat}g_j.\end{aligned} \tag{23}$$

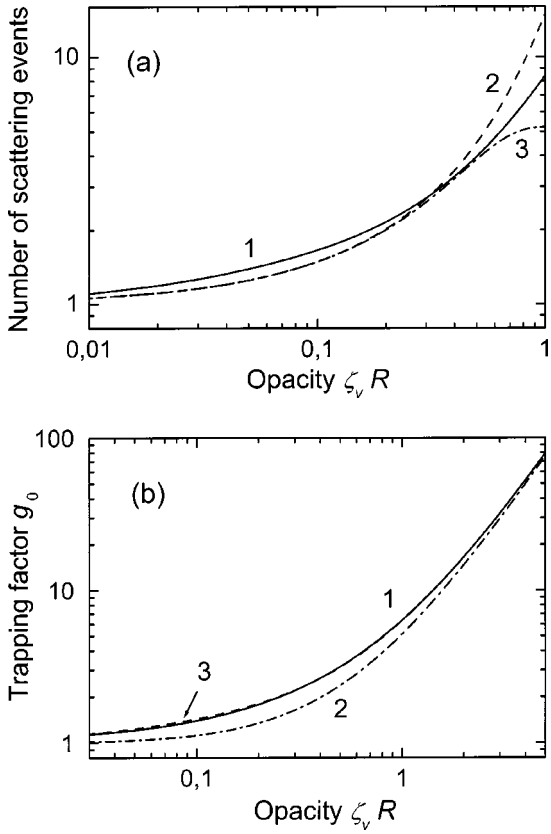

FIG. 3. Trapping characteristics as a function of the opacity $\zeta_v R$ of the atomic beam. (a) Comparison of mean number of scattering events $\overline{N}_v(r_b=0)$ at small opacities obtained by different methods: (1) Solid curve: Fokker–Planck method, Eq. (17). (2) Dashed curve: reciprocal of the Biberman factor $M_{\rm eff}$, Eq. (19). (3) Dot-dashed curve: reciprocal of the series expansion of the Biberman factor, Eq. (20). (b) Trapping factor g_0 of the fundamental mode $j=0$. The solid curve (1) displays the exact g_0 values obtained from Eq. (28) using the exact function $V(p)$, Eq. (26). The dashed-dotted curve (2) corresponds to the g_0 factor evaluated using Fokker–Planck approach determined by approximation (33). The dashed curve (3) presents Fokker–Planck results corrected by introducing a reduced optical thickness. In the scale of the figure curves (1) and (3) practically coincide.

The position-dependent rate constant W_Ω represents a formal quenching process which is introduced for the sake of technical convenience of further calculations. Such a procedure does not influence the above discussion since $W_\Omega(\vec{r})\equiv 0$ within the beam volume Ω_b.

By definition [Eq. (23)], the trapping factors g_j are directly related to the effective lifetimes τ_j of the eigenmodes. They give the number of absorption and reemission events experienced by a photon in the jth mode. The latter decays with a single lifetime $\tau_j=\tau_{\rm eff}(\psi_j(\vec{r}))$. Using Eq. (22), the relation between τ_j and the mean scattering number N_v can be written as

$$g_j=\tau_j/\tau_{\rm nat}=\int_{\Omega_b} d^3r\,\overline{N}_v(\vec{r})\psi_j(\vec{r})\Big/\int_{\Omega_b} d^3r\,\psi_j(\vec{r}). \tag{24}$$

A full solution of the spectral problem defined by Eq. (23) in an atomic beam can be obtained by employing the geometrical quantization technique (GQT).[4,5,27]

C. Solution of the spectral problem using GQT

The basic strategy of GQT lies in exploiting the analogy between the integral Eq. (23) and the stationary wave equation for a classical Hamiltonian system.[4] First, the spectral problem is considered in infinite space Ω_∞, which in our case corresponds to a beam with infinite radius. This is convenient because for infinite space an exact analytical solution is possible. Due to the cylindrical symmetry, the solutions of the integral Eq. (23) do not depend on the coordinate y associated with the beam flow direction: $\psi_j(\vec{r})=\psi_j(x,z)$. These solutions can be represented in a simple form of propagating wave $\psi_{\vec{p}}(\vec{r})=\exp(i\vec{p}\cdot\vec{r})$ of a freely moving particle with momentum $\vec{p}$, which plays a role of a continuous mode index. The dependence on the y coordinate is eliminated by setting $p_y=0$. The momentum $\vec{p}=\{p_x,0,p_z\}$ is thus orthogonal to the beam axis $\vec{e}_y$. As shown in Appendix A, the use of modes $\psi_{\vec{p}}$ reduces the spectral problem (23) to a set of simple algebraic relations

$$\begin{aligned}&\lambda_p\psi_{\vec{p}}(\vec{r})=\Gamma_{\rm nat}V(\vec{p})\,\psi_p(\vec{r})+W_\Omega\psi_p(\vec{r}),\\&V(\vec{p})=1-\int\int\int_{-\infty}^{\infty}dx'\,dy'\,dz'\\&\qquad\times\exp(ip_xx'+ip_zz')G_v(\vec{r}=0,\vec{r}'),\end{aligned}\tag{25}$$

where $V(\vec{p})$ is determined by Fourier transformation of the kernel G_v, Eq. (10). According to Appendix A, its explicit representation is given by

$$\begin{aligned}V(\vec{p})&\equiv V(p)\\&=1-\int_0^{\pi/2}d\theta\sin\theta\frac{1}{\sqrt{1+p^2/\zeta_v^2\sin^2\theta\cos^2\theta}},\\p&=\sqrt{p_x^2+p_z^2}.\end{aligned}\tag{26}$$

Obviously, $V(\vec{p})$ is a function of the absolute value of the momentum $p=|\vec{p}|$ (i.e., of the dimensionless ratio $\tilde{p}=p/\zeta_v$), which reflects the azimuthal symmetry of the RI problem considered here. The integral operator induces a multiplication by the function $V(p)$ in Fourier space and can be considered as a function V of the momentum $\vec{p}$. The latter can be replaced by $\vec{p}=-i\vec{\nabla}$ in the space of $\{x,z\}$ coordinates (i is the imaginary unit).[28] The spectral problem (23) can thus be expressed in an alternative form

$$\lambda_j\psi_j(\vec{r})=\Gamma_{\rm nat}V(-i\vec{\nabla})\,\psi_j(\vec{r})+W_\Omega(\vec{r})\,\psi_j(\vec{r}).\tag{27}$$

We immediately recognize the similarity of the above expression with the generalized stationary Schrödinger equation with Planck constant $\hbar=1$. The ''quantum'' Eq. (27) describes the wave function (mode) $\psi_j(\vec{r})$ of a classical system (the so-called associated quasiparticle[4]) with a uniquely determined Hamiltonian $H(\vec{p},\vec{r})=\Gamma_{\rm nat}V(p)+W_\Omega(\vec{r})$. The function $\Gamma_{\rm nat}V(p)$ gives the ''kinetic energy'' of a quasiparticle, while the quenching rate $W_\Omega(\vec{r})$ corresponds to the ''potential energy.'' With such an interpretation, the effective radiative constants λ_j correspond to the total ''energy'' of the quasiparticle.

In order to preserve the quasiparticle notation under the conditions of finite beam volume Ω_b, the spectral problem (23) should be extrapolated from Ω_b to an infinite space Ω_∞ (Ref. 4). This can be achieved by employing the formal procedure proposed in Ref. 14: the volume Ω_∞ is divided into two parts, such that quenching is absent within Ω_b ($W_\Omega=0$), while outside Ω_b a strong quenching causes fast deactivation of excited states [$W_\Omega(\vec{r})=\infty$]. This construction solves the formulated task since all Na($3p$) atoms disappear immediately outside Ω_b and thus do not affect the excitation of atoms inside the beam. Keeping in mind the interpretation of W_Ω as a potential energy, it is clear that the quasiparticle is confined within a potential well with infinitely high walls created by the atomic beam boundary. Hence the quasiparticle is trapped inside the beam volume Ω_b and experiences elastic reflections from its boundary. The factors λ_j thus become the discrete quantized energy values of the quasiparticle.

From the semiclassical point of view, the solutions of the wave Eq. (27), which determine the eigenstates of the quasiparticle, can be found by imposing appropriate quantization conditions, whereby it is sufficient to consider only the radial dependence of the modes, $\psi_j\equiv\psi_j(r_b)$. The quantized values p_j of the quasiparticle momentum can then be extracted from the Bohr–Sommerfeld quantization rule:[4,28]

$$2\frac{p_j}{\zeta_v}\zeta_vR=2\pi j+\frac{\pi}{2}+\Delta S(p_j),\quad \lambda_j=\Gamma_{\rm nat}V(p_j).\tag{28}$$

Equation (28) has the following physical meaning. Within the volume Ω_b, the Hamiltonian $H=\Gamma_{\rm nat}V(p)$ does not depend on the spatial coordinate $\vec{r}$ ($W_\Omega=0$). Therefore the quasiparticle moves freely ($p_j=$const) within the beam and is reflected from its surface ($r_b=R$) or axis ($r_b=0$). The motion is thus formally restricted to half of the beam diameter $r_b\geqslant 0$. The corresponding wave function (the jth mode) has the form of a standing de Broglie wave[29] with phase $p_jr_b+S_0$. The phase of the quasiparticle jumps at each reflection. It increases by $\Delta S=\pi/2$ at reflection from the beam axis $r_b=0$ (Ref. 28) and by $\Delta S(p_j)$ at reflection from the beam surface[4] (see Fig. 4):

$$\Delta S(p_j)=\frac{\pi}{2}-\frac{2}{\pi}\int_0^1\ln\left(\frac{V(p_j)-V(p_j\xi)}{V(p_j/\xi)-V(p_j)}\right)\frac{1}{1-\xi^2}d\xi.\tag{29}$$

The quantization rule (28) defines resonance conditions for the existence of the jth eigenmode in a ''resonator'' represented by the beam volume Ω_b. The ''allowed'' (resonance) values of the momentum p_j determine the decay rates λ_j via the kinetic energy of the quasiparticle. The longest-living fundamental mode corresponds to the ground state with $j=0$. The Holstein g_0 factor [Fig. 3(b)] is equivalent to $g_0=(\tau_{\rm nat}\lambda_{j=0})^{-1}$.

Using the approximation suggested in Ref. 4, it is straightforward to evaluate the phase shift $\Delta S(p_j)$ in a form convenient for rapid evaluations:

$$\Delta S_{\rm app}(p_j)=\frac{\pi}{2}[1+\gamma_{\rm app}(p_j)],\tag{30}$$

where

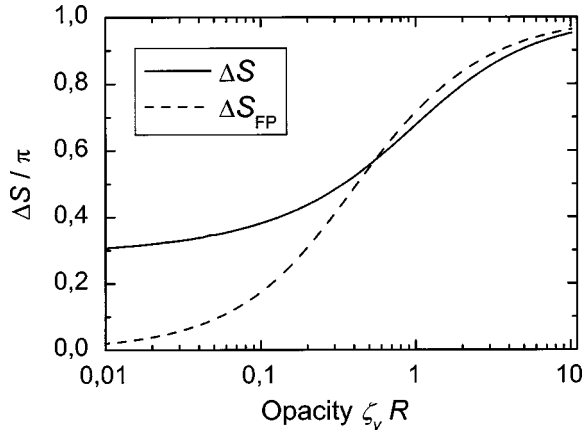

FIG. 4. Phase factor ΔS entering the quantization law, Eq. (28), and accounting for photons escaping from the beam volume without reflection on its boundary. The dashed curve ΔS_{FP} is the Fokker–Planck result for ΔS.

$$\gamma_{\mathrm{app}}(p)=\frac{1}{2}p\frac{d}{dp}\ln\left(p\frac{dV(p)}{dp}\right).$$

Since the function $V(p)$ depends on the dimensionless ratio $\tilde{p}=p/\zeta_v$, Eq. (28) yields a system of equations $\{\lambda_j(\widetilde{p_j}),\chi_v(\widetilde{p_j})\}$ determining the dependence of λ_j on the opacity $\chi_v=\zeta_v R$ in a parametric form comfortable for computational purposes.

D. Solution of the spectral problem using the Fokker–Planck approach

The spectral problem (23) relates uniquely to the imprisonment operator $\hat{G}_v$, Eq. (10). Equation (27) allows the replacement of the imprisonment operator by its alternative representation $\hat{G}_v=\hat{I}-V(-i\vec{\nabla})$. Equation (14) for the mean scattering number $\overline{N}_v$ can then be rewritten as

$$V(-i\vec{\nabla})\overline{N}_v(r_b)=1, \tag{31}$$

where r_b is the distance of point $\vec{r}$ from the beam axis. In the quasiparticle terminology, which was introduced in Sec. IV C, the above equation identifies the integral imprisonment operator with the kinetic energy operator $V(-i\vec{\nabla})$. At large opacities of the beam, the ratio $\tilde{p}=p/\zeta_v$ is small, and the behavior of the function $V(p)$, which is determined by the integral (26), reduces to a simple quadratic power law

$$V(p)|_{\tilde{p}\to 0}=\frac{p^2}{15\zeta_v^2}\Rightarrow V(-i\vec{\nabla})=-\frac{1}{15\zeta_v^2}\Delta, \tag{32}$$

where $\Delta=-\hat{p}^2=\vec{\nabla}^2$ stays for the Laplace operator. In other words, the kinetic energy of quasiparticles simplifies to the usual $\sim p^2$ dependence. Therefore the wave representation $(\vec{p}\to\hat{\vec{p}}=-i\vec{\nabla})$ of quasiparticles justifies the use of the FP approach for the solution of both the steady-state Eqs. (14) and (31) and the spectral problem (23).

However, the asymptotic Eq. (32) does not satisfy the requirement $V(\tilde{p}\to\infty)=1$, which holds for any transparent medium with zero opacity. Indeed, if $\zeta_v R=0$, the photons should be able to escape from the gas without absorption and all trapping factors reach the value of unity. This circumstance can be accounted for by using an approximation

$$V(p)\simeq V_{\mathrm{FP}}(p)\equiv\frac{p^2}{15\zeta_v^2+p^2}\Rightarrow\Delta S_{\mathrm{FP}}(p)=2\arctan\left(\frac{\sqrt{15}\zeta_v}{p}\right). \tag{33}$$

The spectral problem, Eq. (23), $\lambda_j\psi_j(\vec{r})=\Gamma_{\mathrm{nat}}V_{\mathrm{FP}}\times(-i\vec{\nabla})\psi_j(\vec{r})$, is a second-order differential equation with a general solution in the form of standing waves, $\psi_j(r_b)\sim\cos(pR-pr_b-\Delta S_{\mathrm{FP}}/2)$, near the beam boundary. The phase shift $\Delta S_{\mathrm{FP}}(p)$ is uniquely determined by the function V_{FP} via the integral (29) which yields the exact representation (33). From this it follows immediately that all modes ψ_j satisfy the relation (16) (where $\overline{N}_v\to\psi_j$), which we use as the boundary condition (16). Note that the phase $\Delta S(p)$ was derived (see Ref. 4 for details) assuming the absence of reflection of escaping photons from the boundary of the absorbing medium.

With the help of Eq. (33), Eq. (31) determining $\overline{N}_v^{(\mathrm{FP})}$ for the operator V_{FP} is transformed to the form

$$\frac{\hat{p}^2}{15\zeta_v^2+\hat{p}^2}\overline{N}_v^{(\mathrm{FP})}(r_b)=1,\quad \hat{p}^2=-\Delta=-\frac{1}{r_b}\frac{\partial}{\partial r_b}r_b\frac{\partial}{\partial r_b}. \tag{34}$$

This equation has a solution

$$\overline{N}_v^{(\mathrm{FP})}(r_b)=1+\frac{15\zeta_v^2}{\hat{p}^2}|1\rangle\equiv 1+\overline{N}_v^{(\mathrm{large})}(r_b),$$
$$\overline{N}_v^{(\mathrm{large})}=\frac{\sqrt{15}}{2}\zeta_v R+\frac{15}{4}(\zeta_v R)^2\left(1-\frac{r_b^2}{R^2}\right). \tag{35}$$

Obviously, the introduced function $\overline{N}_v^{(\mathrm{large})}$ satisfies the equation $-\Delta\overline{N}_v^{(\mathrm{large})}=15\zeta_v^2$ with the boundary condition (16) and was evaluated already in Sec. III A. Thus the approximation V_{FP} provides indeed a proper extrapolation of the FP solution towards zero opacity of the beam. The accuracy of calculations employing the approximated function V_{FP} instead of $V(p)$ can be judged from Fig. 3(b) where g_0 factors calculated by different methods are compared. These factors determine the lifetime of the fundamental mode and are related to the escape factor in Eq. (1) as $g_0=g^{-1}$. The g_0 value calculated by the FP method reaches the largest discrepancy of 33% from the exact value at opacities $\zeta_v R=0.2$. It occurs due to the rough approximation of the actual phase ΔS, Eq. (29) (Fig. 4, solid curve), by the FP phase ΔS_{FP}, Eq. (33) (Fig. 4, dashed curve). The reason for the disagreement of the two phase factors can be easily seen from the approximation (30). Indeed, for a function $V(p)$ with a power law dependence $V(p)\simeq\alpha+\beta p^{\gamma}$ on the momentum p the phase shift is $\Delta S\simeq\pi/2(1+\gamma/2)$. At large opacities $\tilde{p}=p/\zeta_v\to 0$, and both $V(p)$ and $V_{\mathrm{FP}}(p)$ exhibit the same p^2 behavior [see Eq. (33)], so that $\gamma=2$ and $\Delta S=\Delta S_{\mathrm{FP}}=\pi$. In a nearly transparent media, in contrast, $\tilde{p}\to\infty$. This implies that $V(p)\simeq 1-\beta p^{-1}$ [$\gamma=-1$: see Eq. (26)] and $V_{\mathrm{FP}}(p)\simeq 1-\beta p^{-2}\times(\gamma=-2)$. The corresponding phase shifts $\Delta S\simeq\pi/4$ and

$\Delta S_{\mathrm{FP}} \simeq 0$ differ considerably at opacities $\zeta_\nu R < 0.3$ (see Fig. 4). Therefore it is necessary to introduce a correction to the extrapolation of $\bar{N}_\nu^{(\mathrm{FP})}$, Eq. (35).

We can take advantage of the fact that at small opacities the function $\bar{N}_\nu(r_b)$ varies weakly within the beam volume and replace it with its value in the center of the beam $\bar{N}_\nu(r_b) \approx \bar{N}_\nu(r_b=0)$. The relation between $\bar{N}_\nu$ and the trapping factor g_0 of the fundamental mode can then be immediately established from the integral (24): $g_0 = \bar{N}_\nu(r_b=0)$. The analytically available information on g_0 factors provides an important tool for improvement of the extrapolation of FP results into the region of small opacities. We follow the conventional method described in the literature (e.g., Ref. 17) and rescale the opacity $\zeta_\nu R \to \zeta_\nu \tilde{R}$ by imposing the requirement $g_0(\zeta_\nu R) = g_0^{(\mathrm{FP})}(\zeta_\nu \tilde{R})$. In other words, we replace the actual beam radius R by the reduced radius $\tilde{R}$ for which the evaluation of g_0 factors by the FP approach becomes exact. The calculations yield results which can be quantitatively approximated by Eq. (17). Figure 3(b) shows that the g_0 values obtained using the reduced FP extrapolation (dashed curve 3) excellently agree with the result of exact calculations (solid curve). Figure 3(a) shows the related $\bar{N}_\nu(r_b=0)$ values. One can see that the discrepancy between the results of the Biberman method based on Eq. (19) (dashed curve) and the corrected FP extrapolation, Eq. (17) (solid curve), does not exceed 10%. This latter value is a good estimate of the accuracy of formula (17).

V. EXCITATION DUE TO RADEXT FROM FAST Na($3p_{3/2}$) PHOTOFRAGMENTS

So far we have considered photon emission and absorption processes within the system of slow sodium atoms for an arbitrary opacity of the beam. In the present section we shall apply the above theory to the specific experimental conditions of Paper I. The relatively small opacity of the beam, $\zeta_\nu R \leqslant \kappa_0 R = 0.37$, simplifies the analysis of radiative excitation transfer considerably because it allows an expansion of different photon propagation factors into series of the small parameter $\kappa_0 R$.

The purpose is to determine the extent to which photons emitted by fast Na($3p_{3/2}$) photofragments lead to excitation of Na($3s_{1/2}$) atoms from the primary beam. In order to determine the number of slow excited Na($3p_{3/2}$) atoms created in this way one must obtain the excitation function S^* entering Eq. (11). As will be shown in the next section [see Eq. (52)], it is sufficient to determine the value of S^* in the center of photodissociation zone Ω_{PD}. The volume Ω_{PD} is depicted in Fig. 2 and corresponds to a sphere of radius $R = 0.1\,\mathrm{cm}$. In the center of this volume,

$$I_\nu(\vec{r}=0) = \Gamma_{\mathrm{nat}} \int_{\Omega_{\mathrm{PD}}} d^3r'\, G_\nu(\vec{r}=0,\vec{r}\,')\varepsilon_\nu(\vec{r}\,')n^*_{\mathrm{fast}}, \quad (36)$$

$$G_\nu(\vec{r},\vec{r}\,') = \frac{1}{4\pi|\vec{r}-\vec{r}\,'|^2}\exp(-\kappa_\nu|\vec{r}-\vec{r}\,'|), \quad (37)$$

$$S^*(\vec{r}=0) = \int_{-\infty}^{\infty} d\nu\, \kappa_\nu I_\nu(\vec{r}=0). \quad (38)$$

The excitation function S^* should account for the following conditions. (i) The photons are emitted in the volume Ω_{PD} by the fast Na($3p_{3/2}$) photofragments, while we assume that their concentration n^*_{fast} is constant within the Ω_{PD}. (ii) In the photodissociation process, the Na($3p_{3/2}$) photofragments are formed with a velocity distribution $f_{\mathrm{fast}}(\vec{v})$. Due to the Doppler effect, the photons emitted by the photofragments at point $\vec{r}\,'$ and propagating towards $\vec{r}=0$ (see Fig. 2) have a frequency distribution

$$\varepsilon_\nu(\vec{r}\,') = \lambda \int d^3v\, f_{\mathrm{fast}}(\vec{v})\,\delta(\vec{n}\vec{v} - v_\nu), \quad v_\nu = (\nu-\nu_0)\lambda, \quad (39)$$

which is normalized as $\int d\nu\, \varepsilon_\nu = 1$. The resulting spectral intensity I_ν of radiation exciting the slow Na($3s_{1/2}$) atoms at point $\vec{r}=0$ is formed by photons emitted by photofragments from the entire set of points $\vec{r}\,'$ belonging to the photodissociation zone Ω_{PD}. The factor $G_\nu(\vec{r}=0,\vec{r}\,')$, Eq. (37), accounts for the probability of these photons to reach the center of the zone Ω_{PD} without absorption. Finally, the coefficient κ_ν determines the fraction of incident light with intensity I_ν which is absorbed at $\vec{r}=0$.

The total velocity of photofragments (relative to the mean flow velocity of the beam) results from the velocity $\vec{e}_y v_y$ of the Na_2 molecules in the beam prior to the dissociation and the velocity v_{PD} acquired in the dissociation:

$$\vec{v} = \vec{e}_y v_y + v_{\mathrm{PD}}\tilde{\vec{n}}. \quad (40)$$

The photofragment angular distribution $P(\tilde{\vec{n}})$ is represented to a good approximation by a $\sin^2\theta_{\mathrm{PD}}$ function (see Sec. III A in Paper I): $P(\tilde{\vec{n}}) \sim 1 - (\tilde{\vec{n}}\cdot\vec{e}_z)^2$. We relate $\tilde{\vec{n}}$ to the recoil direction of the excited photofragments. Since the emission profile, Eq. (39), is a function of the scalar product $\vec{n}\cdot\vec{v} = -v_y\cos\theta - v_{\mathrm{PD}}(\tilde{\vec{n}}\cdot\vec{n})$, it is convenient to introduce a new coordinate system $\{\tilde{x},\tilde{y},\tilde{z}\}$ with the new $\tilde{y}$ axis pointing in the direction of $-\vec{n}$ (see Fig. 2). This is done in two steps by Euler transformation. First, the $\{x,z\}$ plane is rotated by an angle φ around the y axis: $\{x,y,z\} \to \{\bar{x},y,\bar{z}\}$. Then the $\{y,\bar{z}\}$ plane is rotated by an angle θ around the $\tilde{x}$ axis: $\{\bar{x},y,\bar{z}\} \to \{\tilde{x},\tilde{y},\tilde{z}\}$. In the new coordinates, the vector $\vec{e}_z$ has the components $\{\cos\varphi\sin\theta, \cos\varphi\cos\theta, -\sin\varphi\}$. In spherical coordinates $\{\tilde{\varphi},\tilde{\theta}\}$ regarding the photofragmentation direction $\tilde{\vec{n}}$, where $\tilde{\vec{n}}$ has the components $\{\cos\tilde{\theta}, \sin\tilde{\theta}\cos\tilde{\varphi}, \sin\tilde{\theta}\sin\tilde{\varphi}\}$, the normalized photofragment angular distribution is written as

$$P(\tilde{\varphi},\tilde{\theta}) = \frac{3}{8\pi}[1-(\tilde{\vec{n}}\cdot\vec{e}_z)^2],$$
$$(\tilde{\vec{n}}\cdot\vec{e}_z) = \cos\tilde{\theta}\cos\varphi\sin\theta + \sin\tilde{\theta}\cos\tilde{\varphi}\cos\varphi\cos\theta - \sin\tilde{\theta}\sin\tilde{\varphi}\sin\varphi. \quad (41)$$

In the new notation, Eq. (39) becomes

$$\varepsilon_\nu(\vec{r}\,') = \lambda \int_{-\infty}^{\infty} dv_y\, f_{\mathrm{mol}}(v_y) \int_0^{2\pi} d\tilde{\varphi} \int_0^{\pi} d\tilde{\theta} \times \sin\tilde{\theta}\, P(\tilde{\varphi},\tilde{\theta})\,\delta(v_\nu + v_{\mathrm{PD}}\cos\tilde{\theta} + v_y\cos\theta),$$

where $f_{\mathrm{mol}}(v_y)$ is the velocity distribution of Na_2 molecules in the beam prior to the dissociation [see Eq. (4)]. After a few direct manipulations this equation can be reduced to the following final form:

$$\varepsilon_\nu(\varphi,\theta)=\frac{\lambda}{\sqrt{\pi}|\cos\theta|\Delta v_{\mathrm{mol}}}\frac{3}{4}\int_{-1}^{1}d\tilde{t}\times\exp\left(-\frac{v_{\mathrm{PD}}^2}{\Delta v_{\mathrm{mol}}^2}\frac{(v_\nu/v_{\mathrm{PD}}+\tilde{t})^2}{\cos^2\theta}\right)\times\left[1-\frac{(1-\tilde{t}^2)}{2}(\cos^2\theta\cos^2\varphi+\sin^2\varphi)-\tilde{t}^2\sin^2\theta\cos^2\varphi\right],\tag{42}$$

where $\tilde{t}=\cos\tilde{\theta}$ and f_{mol} is substituted by its exponential representation (4).

The emission profile ε_ν does not depend on the distance r'. Therefore, after integration of Eq. (36) over r' in spherical coordinates $d^3r'=(r')^2dr'\,d\varphi\,d\theta\sin\theta$, the source function S^* given by Eq. (38) is reduced to

$$S^*(\vec{r}=0)=\Gamma_{\mathrm{nat}}n^*_{\mathrm{fast}}\frac{1}{4\pi}\int_0^{2\pi}d\varphi\int_0^{\pi}d\theta\sin\theta\int_{-\infty}^{\infty}d\nu\,\varepsilon_\nu(\varphi,\theta)\times\left\{1-\exp\left[-\frac{\kappa_0R}{\sqrt{1-\cos^2\theta}}\times\frac{\sqrt{\pi}\Delta v_{\mathrm{at}}}{|\cos\theta|}f_{\mathrm{at}}\left(\frac{v_\nu}{|\cos\theta|}\right)\right]\right\}.\tag{43}$$

For the reasons explained in Sec. VI A, the integration in Eq. (43) is not restricted to the photodissociation zone Ω_{PD} as in Eq. (38), but is performed over the entire beam volume Ω_b. Formally, it corresponds to introducing an additional factor $1/\sqrt{1-\cos^2\theta}$ into the argument of the exponential transmission factor. Such a replacement of the integration volume is justified by the consideration given in Appendix B.

In fact, the photofragment emission profile ε_ν is a convolution of a narrow profile with the width $\lambda^{-1}|\cos\theta|\Delta v_{\mathrm{mol}}$ related to the initial velocity distribution of molecules in the beam [velocity component $\vec{e}_y v_y$ in Eq. (40)] and a broad profile with the width $\lambda^{-1}v_{\mathrm{PD}}$ due to the velocity acquired by fragments in the dissociation [velocity component $v_{\mathrm{PD}}\tilde{\vec{n}}$ in Eq. (40)]. This convolution is complicated by the fact that the velocity distribution is anisotropic with respect to the angular variables. Efficient excitation of slow $Na(3s_{1/2})$ atoms from the primary beam occurs at frequencies ν close to the center of the absorption profile κ_ν, Eq. (6), i.e., for atoms with velocities $v_\nu=(\nu-\nu_0)\lambda\in(-|\cos\theta|\Delta v_{\mathrm{at}},|\cos\theta|\Delta v_{\mathrm{at}})$. Evidently, these frequencies belong to the center of the emission profile ε_ν, which varies insignificantly at frequencies for which κ_ν is high enough to ensure an efficient absorption. The latter can be directly verified by evaluating the integral in Eq. (42). For photodissociation from vibrational levels $v''\geqslant 17$ the ratio $v_{\mathrm{PD}}^2/\Delta v_{\mathrm{mol}}^2$ exceeds the value of $\cong 9$. This allows us to use the saddle point technique in the vicinity of point $\tilde{t}=v_\nu/v_{\mathrm{PD}}$, which yields

$$\varepsilon_\nu(\varphi,\theta)=\frac{3}{4}\frac{\lambda}{v_{\mathrm{PD}}}\left[1-\frac{(1-v_\nu^2/v_{\mathrm{PD}}^2)}{2}(\cos^2\theta\cos^2\varphi+\sin^2\varphi)-\frac{v_\nu^2}{v_{\mathrm{PD}}^2}\sin^2\theta\cos^2\varphi\right].\tag{44}$$

The small values of the ratio $(v_\nu/v_{\mathrm{PD}})^2\leqslant 0.1$ (with $|v_\nu|\leqslant\Delta v_{\mathrm{at}}$) suppress the dependence of ε_ν on the frequency.

Since the opacity κ_0R is small, the source function S^*, Eq. (43), with the emission profile $\varepsilon_\nu(\varphi,\theta)$ given by Eq. (44), can be expanded in series of κ_0R in a manner similar to that used for the calculation of the Biberman escape factor, Eq. (20):

$$S^*(\vec{r}=0)=\Gamma_{\mathrm{nat}}n^*_{\mathrm{fast}}\kappa_0R\frac{15\pi\sqrt{\pi}}{64}\frac{\Delta v_{\mathrm{at}}}{v_{\mathrm{PD}}}\left[1+\frac{1}{8}\frac{\Delta v_{\mathrm{at}}^2}{v_{\mathrm{PD}}^2}+\frac{\sqrt{2}}{\pi}\kappa_0R(\ln(\kappa_0R)-1.75+\mathbf{C})+\cdots\right].\tag{45}$$

Such an expansion is valid for the same range of opacities ($\kappa_0R<0.5$) as in the case of the expansion in Eq. (20). Comparison with the results of numerical evaluation of Eq. (43) shows that Eq. (45) does not differ from the exact expression by more than 3%.

The nonuniformity of the spectral profile ε_ν becomes noticeable at frequencies $|\nu-\nu_0|\sim v_{\mathrm{PD}}/\lambda$ and may somewhat influence the efficiency of RADEXT due to absorption of photons at the wings of the absorption profile κ_ν. To determine this influence, the source function, Eq. (43), should be calculated using the exact profile ε_ν given by Eq. (42). Using the first-order series expansion of the exponential factor on the opacity κ_0R, a number of elementary transformations reduces Eq. (43) to the form

$$S^*(\vec{r}=0)=\Gamma_{\mathrm{nat}}n^*_{\mathrm{fast}}\kappa_0R\frac{\Delta v_{\mathrm{at}}}{\Delta v\sqrt{2}}\frac{3}{32}\int_{-1}^{1}\frac{dt}{|t|\sqrt{1-t^2}}\times\int_{-1}^{1}d\tilde{t}(3-\tilde{t}^2-t^2+3\tilde{t}^2t^2)\exp\left(\frac{v_{\mathrm{PD}}^2}{2\Delta v^2}\frac{\tilde{t}^2}{t^2}\right),\tag{46}$$

with

$$\Delta v^2=\frac{\Delta v_{\mathrm{at}}^2+\Delta v_{\mathrm{mol}}^2}{2}.$$

This equation shows that the properties of RADEXT are determined by a new effective mean velocity Δv. This new variable arises due to the combination of the absorption profile κ_ν with the emission profile ε_ν, Eq. (42), whereby the latter is a product of the convolution of contributions due to the initial velocity distribution of molecules in the beam and the velocity distribution acquired during the fragmentation process. The large value of the ratio $v_{\mathrm{PD}}^2/(2\Delta v^2)\simeq 5$ allows us again to use the saddle point technique for the evaluation of the integrals. After a few manipulations, the final result is

expressed in a form identical with Eq. (45), except that the first two terms in square brackets should be replaced as follows:

$$1+\frac{1}{8}\frac{\Delta v_{\rm at}^2}{v_{\rm PD}^2}\to 1+\frac{1}{4}\rho^2, \quad \rho=\frac{\Delta v}{v_{\rm PD}}. \tag{47}$$

Equation (46) contains helpful information about the course of the excitation process of atoms from the primary beam by photons emitted by excited photofragments. The integrand of Eq. (46) implies that the main contribution to the value of S^* is due to angles $\tilde{\theta}$ with $\cos\tilde{\theta}\equiv\tilde{t}\simeq 0$. This means that the main contribution to the population of the slow Na$(3p)$ atoms is due to photons emitted by photofragments perpendicularly to their fragmentation velocity regardless of the direction of the fragmentation. Indeed, at $|\cos\tilde{\theta}|>0$ the Doppler frequency shift due to the photofragmentation velocity, $|\lambda^{-1}v_{\rm PD}\cos\tilde{\theta}|$, exceeds the absorption width $\lambda^{-1}\Delta v_{\rm at}|\cos\theta|$. Consequently, most of the photons emitted by the photofragments with $|\cos\tilde{\theta}|>0$ leave the primary beam without absorption. This fact is represented by the exponentially decreasing multiplier in Eq. (46). The RADEXT process is thus dominated by $\cos\tilde{\theta}\simeq 0$.

The above-discussed broadband nature of the emission profile allows us to draw definite conclusions about the velocity distribution $\tilde{f}(v_y)$ of the source function entering the kinetic Eq. (7). The probability to excite a slow atom with velocity v_y at point $\vec{r}$ is proportional to the product of the probability $f_{\rm at}(v_y)$ to find an atom with such a velocity and the total intensity $I_{\tilde{\nu}}(\vec{r})$ of the radiation "seen" by this atom. This "seen" intensity depends on the Doppler frequency shift $\tilde{\nu}-\nu_0=\cos\theta v_y/\lambda$. The profile of $I_\nu(\vec{r})$, Eq. (36), is not necessarily identical with the profile ε_ν given by Eq. (39). The exponential transmission factor $\exp(-\kappa_\nu|\vec{r}-\vec{r}'|)$ in Eq. (37) implies that during the propagation of photons from the emission point $\vec{r}'$ to the absorption point $\vec{r}$ they are absorbed in the beam volume with an efficiency depending on their frequency ν. However, since the opacity $\kappa_0 R$ is small, the transmission factor is close to unity. Therefore the intensity profile $I_\nu(\vec{r})$ follows the broadband character of the emission profile ε_ν, Eq. (44). Consequently, the RADEXT process leads to a velocity distribution of the source function close to that of the ground-state atoms in the beam, $\tilde{f}(v_y)\simeq f_{\rm at}(v_y)$. To illustrate this conclusion, we examine the expression for the velocity distribution of the source function in the center of the photodissociation zone: $\tilde{f}(v_y)\sim f_{\rm at}(v_y)I_{\tilde{\nu}}|_{\vec{r}=0}$. Inserting Eq. (44) into Eq. (36) and integrating the latter over the radius r' and angle φ in the spherical coordinate system $\{r',\theta,\varphi\}$, we obtain

$$\tilde{f}(v_y)|_{\vec{r}=0}\sim f_{\rm at}(v_y)\frac{3}{4}\int_{-1}^{1}dt\left[1-\frac{(1-v_y^2/v_{\rm PD}^2)}{4}(1+t^2)-\frac{v_y^2}{2v_{\rm PD}^2}(1-t^2)\right]\frac{1-\exp(-\zeta_v R/|t|)}{\zeta_v R/|t|}. \tag{48}$$

Here $t=\cos\theta$ and the absorption factor ζ_v is determined by Eq. (10). The calculations show (see Fig. 5) that for the opacity $\kappa_0 R=0.37$ the profile of the distribution function

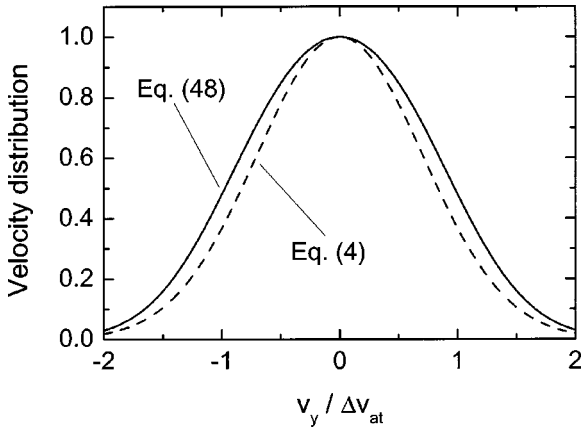

FIG. 5. Solid curve: velocity distribution $\tilde{f}(v_y)|_{\vec{r}=0}$, Eq. (48), of the source function in the center of the photodissociation zone $\Omega_{\rm PD}$. Dashed curve: initial Maxwellian velocity distribution $f_{\rm at}(v_y)$, Eq. (4), of ground-state atoms in the beam. In the figure both functions are normalized to unity at $v_y=0$.

$\tilde{f}(v_y)|_{\vec{r}=0}$ deviates only slightly from the Maxwellian function $f_{\rm at}(v_y)$. The widths of the distributions $f_{\rm at}$ and $\tilde{f}$ are $\Delta v=\Delta v_{\rm at}$ and $\widetilde{\Delta v}=1.19\,\Delta v_{\rm at}$, respectively: i.e., they differ by only 19%. We define the width Δv of any symmetrical velocity distribution function $f(v)$ as $\Delta v^2=2\int dv\, v^2 f(v)/\int dv\, f(v)$.

VI. RESULTS AND DISCUSSION

A. Total number of slow Na$(3p_{3/2})$ atoms produced by RADEXT

In the preceding sections we have obtained the set of equations necessary for the calculation of the total number $N_{\rm Na^*_{slow}}$ of slow Na$(3p_{3/2})$ atoms created due to RADEXT. In order to obtain a numeric result describing the process under the conditions of Paper I, Eq. (13) should first be averaged over the normalized velocity distribution $\tilde{f}(v)$ [Eq. (8)] of the source function $S^*(\vec{r},v_y)$:

$$N_{\rm Na^*_{slow}}=\Gamma_{\rm nat}^{-1}\int_{\Omega_b}d^3r\,S^*(\vec{r})\overline{N}(\vec{r}), \quad \overline{N}(\vec{r})\equiv\overline{N}(r_b), \tag{49}$$

$$\overline{N}(r_b)=\langle\overline{N}_v(r_b)\rangle \simeq 1+\frac{\sqrt{15}}{2}\frac{\kappa_0\tilde{R}}{\sqrt{2}}+\frac{15}{4}\frac{(\kappa_0\tilde{R})^2}{\sqrt{3}}\left(1-\frac{r_b^2}{\tilde{R}^2}\right), \tag{50}$$

$$\kappa_0\tilde{R}=\kappa_0 R\left(1+\frac{1}{0.2+5.47\kappa_0 R+0.169(\kappa_0 R)^2}\right). \tag{51}$$

In Eq. (50) we have taken into account that averaging the coefficients entering Eq. (17) yields $\langle\zeta_v\rangle=\kappa_0/\sqrt{2}$ and $\langle\zeta_v^2\rangle=\kappa_0^2/\sqrt{3}$. We have ignored the averaging of the rescaled beam radius $\tilde{R}$ over the distribution $\tilde{f}(v)$ and use instead the value of $\tilde{R}$ from Eq. (17) for $v=0$. Such an approximation of the correction factor $\kappa_0\tilde{R}$ does not introduce a significant inaccuracy. The values of N determined using Eq. (50) and the exact expression, Eq. (17), do not differ by more than 6% [see below the numeric example for $\langle\overline{N}_v(r_b=0)\rangle$].

Since the source function $S^*(\vec{r})$ is mainly localized within the photodissociation zone Ω_{PD}, where both $S^*(\vec{r})$ and $\overline{N}(r_b)$ are slowly varying functions of their arguments, the integral (49) can be approximated by the relation

$$N_{\mathrm{Na}^*_{\mathrm{slow}}} = \Omega_{\mathrm{PD}} S^*(\vec{r}=0)\,\frac{\overline{N}(r_b=0)}{\Gamma_{\mathrm{nat}}} = N_{\mathrm{Na}^*_{\mathrm{fast}}}\,\frac{S^*(\vec{r}=0)}{n^*_{\mathrm{fast}}}\,\frac{\overline{N}(r_b=0)}{\Gamma_{\mathrm{nat}}}, \tag{52}$$

where we have assumed that the density n^*_{fast} of the excited photofragments does not vary within the photodissociation zone Ω_{PD}, so that $N_{\mathrm{Na}^*_{\mathrm{fast}}} = n^*_{\mathrm{fast}}\Omega_{\mathrm{PD}}$. Note that n^*_{fast} in the denominator on the right-hand side of Eq. (52) cancels out when the expression for the source function $S^*(\vec{r}=0)$ is inserted, since the latter also contains the term n^*_{fast} [see Eq. (45)].

Strictly speaking, the source function $S^*(\vec{r})$ extends beyond the photodissociation zone Ω_{PD}. This is because the photons emitted by the fast Na($3p_{3/2}$) photofragments can be absorbed in the entire volume Ω_b of the beam and not only within Ω_{PD}. To account for this fact, we have replaced in Eq. (38) the integration over the zone Ω_{PD} by the integration over the beam volume Ω_b [see the remark just after Eq. (43)]. The analysis of Eq. (49) given in Appendix B justifies such a replacement. Moreover, this analysis shows also that the total number of fast Na($3p_{3/2}$) photofragments entering Eq. (52) does not depend on the particular shape of the photodissociation zone, which is chosen as a sphere in the above treatment. Furthermore, it does not depend on the particular spatial distribution of the fast photofragments, because the term $S^*(\vec{r}=0)/n^*_{\mathrm{fast}} = \tilde{\Phi}(\vec{r}\,'=0)$ does not depend on n^*_{fast} [see Eq. (B4)]. Therefore the assumption $n^*_{\mathrm{fast}} = \mathrm{const}$, which was done when calculating the integrals in Eqs. (38) and (36), does not influence the accuracy of the result. Thus Eq. (52) is valid for realistic experimental conditions which usually involve an intensity distribution within the laser beam and a photodissociation zone which usually does not have a spherical shape. The accuracy of Eq. (52) is only restricted by the assumption of a slow variation of the function $\overline{N}(r_b)$, Eq. (50), with the spatial coordinate r_b. Figure 3(a) shows the range of beam opacities for which Eq. (52) is applicable: the mean number of scattering events (solid curve) must be approximately equal to the reciprocal of the Biberman factor M_{eff} (dashed curve). This condition is fulfilled for opacities $\kappa_0 R < 0.5$.

Under the conditions of the experiment of Paper I, $\kappa_0 R = 0.37$, $\Delta v_{\mathrm{at}} = 300$ m/s, $\Delta v_{\mathrm{mol}} = 260$ m/s, and $\Delta v = 281$ m/s, and according to Eqs. (50) and (51), we obtain $\overline{N}(r_b=0) = 2.35$. In the context of Paper I, the value $\overline{N}(r_b=0)$ relates to the escape factor g in Eq. (1) as $\overline{N}(r_b=0) = 1/g$. It is interesting to compare the $\overline{N}(r_b=0)$ value with the result of exact averaging, $\langle \overline{N}_v(r_b=0)\rangle = 2.50$, given by Eq. (17). Hence Eqs. (50) and (51) can be considered as sufficiently accurate.

Finally, incorporating Eq. (45) into Eq. (52) and accounting for the correction (47), we obtain for the given geometry of Paper I (when the photodissociating laser is polarized perpendicularly to the beam axis) that the ratio of the number of slow atoms produced in the RADEXT to the number of fast photofragments produced in the dissociation can be expressed as

$$\frac{N_{\mathrm{Na}^*_{\mathrm{slow}}}}{N_{\mathrm{Na}^*_{\mathrm{fast}}}} = \overline{N}(r_b=0)\,\kappa_0 R\,\frac{15\pi\sqrt{\pi}}{64}\,\frac{\Delta v_{\mathrm{at}}}{v_{\mathrm{PD}}}\left[1+\frac{1}{4}\rho^2 + \frac{\sqrt{2}}{\pi}\,\kappa_0 R[\ln(\kappa_0 R) - 1.75 + \mathbf{C}]\right], \quad \rho = \frac{\Delta v}{v_{\mathrm{PD}}}. \tag{53}$$

Inserting the values of photofragment velocities $v_{\mathrm{PD}}(v''=17) = 857$ m/s and $v_{\mathrm{PD}}(v''=23) = 1065$ m/s, we obtain for the ratio (53) the values of 0.26 and 0.21 for photodissociation from the levels $v''=17$ and $v''=23$, respectively. Although these values are in fairly good agreement with the experimental results (see Table I), they still show a reversed tendency: the theoretical ratio is larger for dissociation from the lower vibrational level, whereas the experimental ratio is larger for dissociation from the higher vibrational level.

TABLE I. Experimental and theoretical data on the ratio of slow to fast Na($3p_{3/2}$) atoms for photodissociation from the vibration levels $v''=17$ and $v''=23$.

	$N_{\mathrm{Na}^*_{\mathrm{slow}}}/N_{\mathrm{Na}^*_{\mathrm{fast}}}$		
Na_2 v'' level	Experiment	RADEXT theory without HFS	RADEXT theory with HFS
17	0.16	0.26	0.13
23	0.22	0.21	0.19

It is worth mentioning that the efficiency of the RADEXT depends on the polarization of the photodissociating laser radiation. Formulas (45) and (53) were obtained for the situation when the photodissociation laser is polarized perpendicularly to the particle beam axis. When the laser is polarized parallel to the beam axis, the term $(\tilde{\vec{n}}\cdot\vec{e}_z)$ in Eq. (41) should be replaced by $(\tilde{\vec{n}}\cdot\vec{e}_y) = \cos\theta\cos\tilde{\theta} - \sin\theta\sin\tilde{\theta}\cos\tilde{\varphi}$. The source function then becomes

$$S^{*(\parallel)}(\vec{r}=0) = \Gamma_{\mathrm{nat}} n^*_{\mathrm{fast}} \kappa_0 R\,\frac{9\pi\sqrt{\pi}}{32}\,\frac{\Delta v_{\mathrm{at}}}{v_{\mathrm{PD}}}\left[1-\frac{5}{12}\rho^2 + \frac{\sqrt{2}}{\pi}\,\kappa_0 R[\ln(\kappa_0 R) - 1.75 + \mathbf{C}]\right]. \tag{54}$$

This leads to an increase in the mean absorption by a factor of 1.2 due to the increase of the fraction of radiation emitted by photofragments in the direction perpendicular to the particle beam axis.

B. Account for the hyperfine structure of Na

So far, we have ignored the hyperfine structure (HFS) of the Na energy levels. In the $3p_{3/2}$ state the hyperfine splitting is relatively small, but it is not so for the ground state $3s_{1/2}$, where the 1772-MHz separation between the $F=1$ and $F=2$ levels is of an order of Doppler shifts in the emission by

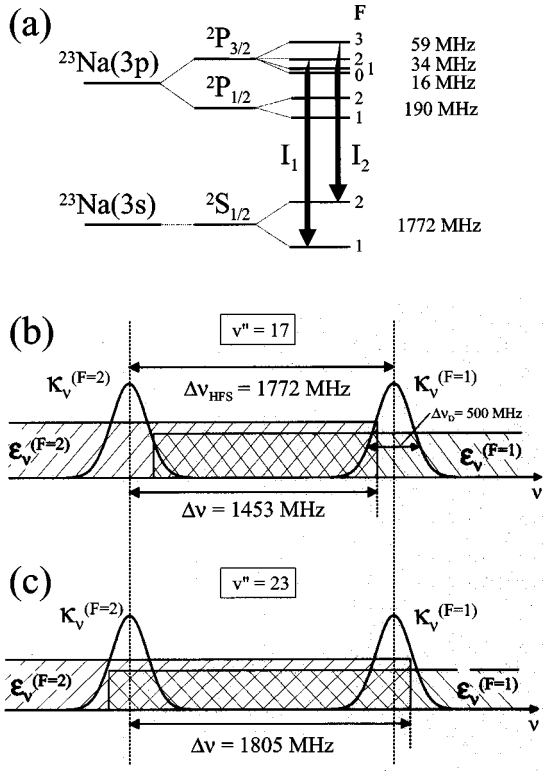

FIG. 6. Hyperfine structure of Na and its influence on the efficiency of RADEXT. (a) Hyperfine splitting of $3p_{3/2}$ and $3s_{1/2}$ levels and the respective splitting of the sodium D_2 spectral line. (b) Emission profiles $\varepsilon_\nu^{(F)}$ of fast photofragments and absorption profiles $\kappa_\nu^{(F)}$ of slow Na atoms for transitions between $3p_{3/2}$ and $3s_{1/2}$ $(F=1,2)$ levels at photodissociation from the vibration level $v''=17$. (c) The same as (b) for the dissociation from $v''=23$.

fast photofragments [see Fig. 6(a)]. Obviously, such large splitting is influencing the radiation imprisonment process and, hence, the efficiency of RADEXT. Here we shall provide a brief insight into this problem and give a simple quantitative evaluation. A detailed account requires the understanding of how the different F sublevels of the $3p_{3/2}$ state are populated in the potodissociation process, and it will be given in a separate publication.

The hyperfine splitting in the excited $3p_{3/2}$ state is much smaller than the Doppler width $\Delta\nu_D=\Delta v_{\rm at}/\lambda=500$ MHz (Fig. 6). Therefore the $3p_{3/2}$ state can be considered as a single energy level, whereby we assume that in the photodissociation the $F=\{0,1,2,3\}$ sublevels are uniformly populated according to their statistical weights. The 1772-MHz hyperfine splitting of the ground state $3s_{1/2}$, in contrast, requires that it is treated as two separate levels $F=1$ and $F=2$ with statistical weights $\bar{g}_1=3$ and $\bar{g}_2=5$, respectively. Therefore the $3p_{3/2}\rightarrow 3s_{1/2}$ transition splits into two spectrally resolved lines [see Fig. 6(a)] with intensities in accordance with the sum rules:[30] $I_1/I_2=\bar{g}_1/\bar{g}_2=3/5$. Furthermore, the sum rules imply that the absorption coefficient in the center of the lines I_1 and I_2 is expressed as a fraction of the coefficient κ_0 given by Eq. (6): $\kappa_0^{(1)}=3/8\kappa_0$ and $\kappa_0^{(2)}=5/8\kappa_0$. An immediate consequence of the hyperfine splitting is the decrease of the effective opacity of the media to the value $\kappa_0^{\rm eff}R\simeq\sqrt{15}/8\kappa_0 R=0.19$ (see Appendix C for quantitative estimates). Accordingly, the escape factor $\bar{N}(r_b=0)$, which is determined by Eq. (50), reduces to $\bar{N}^{(\rm eff)}(r_b=0)=1.8$. This, in turn, leads to a decrease of the ratio of numbers of slow and fast Na$(3p)$ atoms, since $\bar{N}(r_b=0)$ enters Eqs. (52) and (53).

Another important manifestation of the effect of HFS is the modification it implies on the source function $S^*(\vec{r}=0)$. Figures 6(b) and 6(c) illustrate how the broadband emission profiles $\varepsilon_\nu^{(F)}$ interact with the absorption profiles $\kappa_\nu^{(F)}=\kappa_0^{(F)}/|\cos\theta|\exp\{-(\nu-\nu_0^{(F)})^2/(\Delta\nu_D|\cos\theta|)\}$, with $F=1,2$. We assume that the Doppler broadening of the emission profile of fast photofragments is due to the velocity $v_{\rm PD}$ they acquire in the dissociation. The width $\Delta v_{\rm mol}$ of the velocity distribution of molecules in the beam is several times smaller than $v_{\rm PD}$ and is restricted to the direction along the y axis. Therefore we disregard its contribution in the following estimates. It means that in the evaluation of $\varepsilon_\nu^{(F)}$ [Eq. (39)] we ignore the low-velocity components v_y in Eq. (40). Furthermore, we neglect the anisotropy in the photofragment angular distribution and optical pumping between the HFS levels of the ground state. The latter can be safely disregarded because the radiation emitted by fast photofragments is very weak compared to the saturation intensity. With such assumptions, the emission profile can be written as

$$\varepsilon_\nu^{(F)}=\begin{cases}\dfrac{\lambda}{2v_{\rm PD}} & \text{when } |\nu-\nu_0^{(F)}|<v_{\rm PD}/\lambda,\\ 0 & \text{when } |\nu-\nu_0^{(F)}|>v_{\rm PD}/\lambda.\end{cases}\tag{55}$$

This equation describes a uniform frequency distribution of emitted photons within the boundaries $\Delta\nu=\pm v_{\rm PD}/\lambda$, where the boundaries correspond to recoil of photofragments towards and backwards from the center of the photodissociation zone (see Fig. 2).

In the case of photodissociation from the vibrational level $v''=17$ with $v_{\rm PD}=857$ m/s, each emission profile $\varepsilon_\nu^{(F)}$, $F=1,2$, extends from the hyperfine line center $\nu_0^{(F)}$ by $\Delta\nu=\pm 1453$ MHz and does not reach the absorption frequencies of the other hyperfine component [see Fig. 6(b)]. Therefore the formation of the source function via RADEXT is independent for both hyperfine components. The resulting effective source function is then given by the sum of source functions for each hyperfine component: $S^*_{\rm eff}(\vec{r}=0)=S^*_1(\vec{r}=0)+S^*_2(\vec{r}=0)$, where S^*_F is defined by Eq. (45), except that κ_0 should be replaced by $\kappa_0^{(F)}$ and $\Gamma_{\rm nat}$ by $\Gamma_{\rm nat}^{(F)}=\bar{g}_F/8\Gamma_{\rm nat}$ to account for branching of the $3p_{3/2}\rightarrow 3s_{1/2}$ transition into hyperfine components. Accordingly, the ratio (53) of numbers of slow and fast excited atoms should be rewritten to account for the two independent HFS contributions:

$$\left.\frac{N_{\rm Na^*_{slow}}}{N_{\rm Na^*_{fast}}}\right|_{\rm eff}=\left.\frac{N_{\rm Na^*_{slow}}}{N_{\rm Na^*_{fast}}}\right|_1+\left.\frac{N_{\rm Na^*_{slow}}}{N_{\rm Na^*_{fast}}}\right|_2,\tag{56}$$

where

$$\left.\frac{N_{\mathrm{Na}^*_{\mathrm{slow}}}}{N_{\mathrm{Na}^*_{\mathrm{fast}}}}\right|_F = \overline{N}^{(\mathrm{eff})}(r_b=0)\,\frac{\overline{g}_F\kappa_0^{(F)}}{8}R\,\frac{15\pi\sqrt{\pi}}{64}\,\frac{\Delta v_{\mathrm{at}}}{v_{\mathrm{PD}}} \times\left[1+\frac{1}{4}\rho^2+\frac{\sqrt{2}}{\pi}\,\kappa_0^{(F)}R[\ln(\kappa_0^{(F)}R)-1.75+\mathbf{C}]\right]. \tag{57}$$

Using Eqs. (56) and (57), we obtain $N_{\mathrm{Na}^*_{\mathrm{slow}}}/N_{\mathrm{Na}^*_{\mathrm{fast}}}=0.13$ for $v''=17$.

In the case of dissociation from the level $v''=23$, the larger fragmentation velocity of $v_{\mathrm{PD}}=1065$ m/s increases the width of the photofragment emission profile $\varepsilon_\nu^{(F)}$, Eq. (55), to $\Delta\nu=\pm 1805$ MHz [see Fig. 6(c)]. This shift is larger than the 1772-MHz splitting between the $F=1$ and $F=2$ HFS levels, so that a fraction of photons emitted on one hyperfine transition can be absorbed on the other. This results in an increased opacity of the medium. Therefore the term $\overline{g}_F\kappa_0^{(F)}/8$ on the right-hand side of Eq. (57) should be replaced by $\overline{g}_F\kappa_0/8$. Furthermore, since the term in the square brackets of Eq. (57) containing $\kappa_0^{(F)}R$ does contribute to no more than 15% of the total value under the conditions of Paper I with $\kappa_0^{(F)}R\simeq\kappa_0^{\mathrm{eff}}R=0.19$, we replace it by an effective value $\kappa_0^{(\mathrm{eff})}R$ common for both HFS components. Summation according to Eq. (56) then yields

$$\left.\frac{N_{\mathrm{Na}^*_{\mathrm{slow}}}}{N_{\mathrm{Na}^*_{\mathrm{fast}}}}\right|_{\mathrm{eff}} = \overline{N}^{(\mathrm{eff})}(r_b=0)\,\kappa_0 R\,\frac{15\pi\sqrt{\pi}}{64}\,\frac{\Delta v_{\mathrm{at}}}{v_{\mathrm{PD}}}\left[1+\frac{1}{4}\rho^2+\frac{\sqrt{2}}{\pi}\,\kappa_0^{(\mathrm{eff})}R[\ln(\kappa_0^{(\mathrm{eff})}R)-1.75+\mathbf{C}]\right]. \tag{58}$$

Inserting the corresponding values we obtain $N_{\mathrm{Na}^*_{\mathrm{slow}}}/N_{\mathrm{Na}^*_{\mathrm{fast}}}=0.19$ for $v''=23$. Comparing the obtained values with the experimental data (see Table I), one can see that the account for the hyperfine structure correctly reproduces the tendency observed in the experiment, with the ratio being smaller for $v''=17$ and larger for $v''=23$. Note that the increase in the ratio for $v''=23$ is explained solely by the fact that the fragmentation velocity has become large enough to shift the emission profile as far as the hyperfine splitting of the ground state. A further increase in the fragmentation velocity due to increased v'' does not lead to any further increase in the RADEXT efficiency as soon as both hyperfine transition frequencies are covered by the photofragment emission. Instead, a monotonic decrease is expected because of the decrease ($\sim 1/v_{\mathrm{PD}}$) in the spectral density of the emission intensity.

VII. CONCLUSION

In the present paper we have provided a theoretical description of radiation trapping in collimated atomic beams. It shows how the effective lifetime of an ensemble of atoms relates to the natural decay rate Γ_{nat}. The trapping factor g_0, which contains quantitative information about the increase of the effective lifetime in an optically thick medium, depends on a number of experimental conditions. Equation (13) implies that the total number of excited atoms, N_v^*, created by the source function S^* depends on its position in space. The total number N_v^* can be directly obtained from the mean number of scattering events, $\overline{N}_v(\vec{r})$, using Eq. (13). The latter number describes the scattering of resonance photons under steady-state conditions in an atomic beam, and we have expressed it analytically by means of the Fokker–Planck technique. Although this method is precise only at large opacities of the beam, an accurate extrapolation of the FP solution into the region of small opacities was achieved by introducing a correction. In essence, this correction means that the actual beam radius is replaced by reduced one. A mathematical justification of this procedure is provided by analysis of the time-dependent radiation imprisonment equation using the geometric quantization technique which was originally developed in Ref. 4. This method introduces a quasiparticle and relates the trapping factors to dynamical characteristics (Hamiltonian) of the quasiparticle in an infinite coordinate space. Essentially, the imprisonment problem in a finite volume of absorbing medium is reduced to the solution of a Schrödinger Eq. (27) for the quasiparticle moving in an effective potential well determined by the atomic beam boundary. Using the semiclassical approach, the trapping factors g_j are obtained as quantized eigenvalues of the quasiparticle Hamiltonian.

The above theory considers ideally collimated beams and neglects any deviation of the particle velocity vectors from the beam axis. The effects of finite but small collimation angles ϑ occurring under realistic experimental conditions become noticeable at large beam opacities. In our theory these effects can be quantitatively accounted for by introducing a diffusion mechanism of excitation transfer between the atoms belonging to different subensembles Ξ_v with fixed velocities v. The velocity conservation within a chosen subensemble Ξ_v is similar to the conservation of frequency during scattering of light in a monochromatic scattering medium. The theory of Milne[1] anticipates that under such conditions the escape factors are proportional to the square of the opacity of the medium, $g_0\sim(\kappa_0 R)^2$. This is represented by the last term on the right-hand side of Eq. (50). The migration of excitation among different subensembles Ξ_v due to the radiative excitation transfer is similar to the frequency diffusion in spectral lines known in the conventional radiation imprisonment treatments as partial frequency redistribution (see Ref. 17 for details). In the media like thermal vapors or poorly collimated effusive beams the exchange with photons among the subensembles Ξ_v becomes very efficient and a complete frequency redistribution dominates. Under such condition the Holstein's law $g_0\sim\kappa_0 R$ applies,[8,9] reducing considerably the efficiency of the radiative excitation transfer. An appropriate modification of geometrical quantization technique allowing the analytical description of radiation imprisonment in beams with $\vartheta>0$ is possible on the base of methods developed in Refs. 27 and 31.

We have applied the developed theory of radiation imprisonment in beams to explain the recently observed phenomenon of radiative excitation transfer (3) discussed in Paper I. In this process, the photons emitted by fast excited photofragments excite atoms from the primary beam with

astonishing efficiency, leading to considerable changes in the velocity distribution of excited atoms after the photodissocion. Using the theory described in this paper, we have shown that such redistribution of the velocities of excited atoms can be well explained by the consequences of radiation trapping. In particular, an interesting conclusion follows from the excitation source function in Sec. V: the major contribution to the excitation of atoms from the primary beam is due to the photons emitted by photofragments perpendicularly to their fragmentation direction, whereby this statement is valid regardless of the direction of the photofragmentation direction.

We have shown that in order to correctly reproduce the experimental observations, the non-negligible hyperfine splitting of the Na ground state should be taken into consideration. Comparison of the results showed an excellent agreement of the predictions of our theory with the experimental data of Paper I. The effect of hyperfine structure on radiation imprisonment has not yet been duly considered in the scientific literature. A detailed study dealing with this matter is in progress and will be reported elsewhere. In conclusion, we emphasize the importance of a proper account of the radiation trapping phenomenon in any experiment involving atoms in resonance states, be they among the initial reactants or the reaction end products.

ACKNOWLEDGMENTS

This work was supported by the Deutsche Forschungsgemeinschaft. One of the authors (A.E.) was supported by EU Marie Curie Individual Fellowship Grant No. HPMF-CT-1999-00080. Partial support by Grant No. INTAS-2001-155, NATO Collaboration Linkage Grant No. PST.CLG.979120, and the Russian Foundation for Basic Research, Project No. 02-02-16586, is also acknowledged. We thank H. Hotop for helpful discussions.

APPENDIX A: FOURIER TRANSFORM OF THE RI EQUATION IN AN INFINITE BEAM

In the GQT, we must consider the spectral problem described by Eq. (23) for a model beam with infinite radius $R=\infty$. We are interested in the action of the RI operator $\hat{G}_v$, which is determined by the integral term of Eq. (9), on the mode $\psi_{\vec{p}}(\vec{r})=\exp(ip_x x+ip_z z)$. Two conditions allow the simplification of the corresponding Fourier integral: (i) $\hat{G}_v$ is a convolution-type operator regarding the $\{x,z\}$ coordinates and (ii) the modes of interest do not depend on y. From (i) it follows that the modes $\psi_{\vec{p}}(\vec{r})$ are eigenfunctions of the operator $\hat{I}-\hat{G}_v$. Their eigenvalues are given by the Fourier transform $V(\vec{p})$, Eq. (25), of the kernel G_v, Eq. (10), over the $\{x',z'\}$ plane, while condition (ii) implies that this transform does not depend on the coordinate y. For convenience, we choose the latter as $y=0$ (see Fig. 2).

In the evaluation of $V(\vec{p})$, Eq. (25), it is convenient to introduce a new coordinate system $\{x',y',z'\}$ which is centered in the photodissociation zone Ω_{PD} (Fig. 2) with the z' axis pointing along the direction of the momentum $\vec{p}=\{p_x,p_z\}$. We then determine spherical coordinates $\{r',\varphi',\theta'\}$ with θ' being the angle between the z' axis and the vector $\vec{r}'$, and φ' being the angle between the y' axis and the projection of $\vec{r}'$ on the $\{x',y'\}$ plane. Such a choice of coordinates allows one to obtain the simplest representation of both the phase factor $p_x x'+p_z z'=|\vec{p}|r'\cos\theta'$ and the factor $\cos\theta=\sin\theta'\cos\varphi'$ which are entering the exponent in Eq. (25) and the kernel G_v Eq. (10). With the above coordinates, the integration of Eq. (25) over the radial coordinate r' reduces it to the form

$$V(\vec{p})=1-\frac{1}{4\pi}\int_0^{\pi}d\theta'\,\sin\theta'\int_0^{2\pi}d\varphi'\times\frac{1}{1+p^2/\zeta_v^2\sin^2\theta'\cos^2\theta'\cos^2\varphi'},\qquad p=\sqrt{p_x^2+p_z^2}. \tag{A1}$$

The integral over φ' is given in Ref. 23:

$$\int_0^{2\pi}d\varphi'\frac{1}{1+\lambda^2\cos^2\varphi'}=\frac{2\pi}{\sqrt{1+\lambda^2}},$$

so that representation (A1) is equal to formula (26).

APPENDIX B: DERIVATION OF EQ. (55)

Consider Eq. (49) determining the total number of slow $\mathrm{Na}(3p_{3/2})$ atoms. Due to the small opacity $\kappa_0 R\leqslant 0.5$, the mean number of scattering events, $N(r_b)$, within the beam changes very little with increasing distance r_b from the beam axis. Therefore it is possible to replace $N(r_b)$ by its value $\overline{N}(r_b=0)$ in the center of the beam:

$$N_{\mathrm{Na}^*_{\mathrm{slow}}}=\Gamma_{\mathrm{nat}}^{-1}\overline{N}(r_b=0)\overline{S^*},\quad \overline{S^*}=\int_{\Omega_b}d^3r\,S^*(\vec{r}). \tag{B1}$$

Inserting Eqs. (36), (37), and (38) in the above equation, the integral value $\overline{S^*}$ of the source function $S^*(\vec{r})$ is obtained by integrating the emission term over the photodissociation volume Ω_{PD} and the absorption term over the beam volume Ω_b:

$$\overline{S^*}=\Gamma_{\mathrm{nat}}\int_{-\infty}^{\infty}d\nu\int_{\Omega_b}d^3r\,\kappa_\nu(\vec{r}-\vec{r}')\times\int_{\Omega_{\mathrm{PD}}}d^3r'\,G_\nu(\vec{r},\vec{r}')\varepsilon_\nu(\vec{r}'-\vec{r})n^*_{\mathrm{fast}}(\vec{r}'). \tag{B2}$$

Importantly, the emission profile ε_ν, Eq. (39), and the absorption profile κ_ν, Eq. (5), depend on the direction $\vec{n}$ between the points $\vec{r}'$ and $\vec{r}$, but not on the spatial positions of $\vec{r}$ or $\vec{r}'$ in the beam. This is a consequence of two properties of the considered experimental situation: (i) the distribution of the ground-state atoms in the beam is to a good approximation homogeneous and (ii) the velocity distribution $f_{\mathrm{fast}}(\vec{v})$ of the $\mathrm{Na}(3p_{3/2})$ photofragments does not depend on the intensity of the photodissociation laser (weak excitation limit). The latter assertion is important because the intensity varies across the laser beam diameter.

Equations (5) and (39) imply that the spectral coefficients ε_ν and κ_ν are symmetrical functions of spatial coordinates. Therefore, after changing the order of integration, Eq. (B2) can be rewritten in the form

$$\overline{S^*}=\Gamma_{\rm nat}\int_{\Omega_{\rm PD}} d^3r'\, n^*_{\rm fast}(\vec{r}\,')\Phi(\vec{r}\,'),$$

$$\Phi(\vec{r}\,')=\int_{-\infty}^{\infty} d\nu \int_{\Omega_b} d^3r\, G_\nu(\vec{r},\vec{r}\,')\kappa_\nu(\vec{r}-\vec{r}\,')\varepsilon_\nu(\vec{r}\,'-\vec{r}). \quad \text{(B3)}$$

The dimensionless function $\Phi(\vec{r}\,')$ has a meaning of some generalized escape factor. The properties of functions of this kind have been studied in Refs. 21 and 27, where it was shown that their dependence on the spatial coordinates is very similar to that for the Biberman factor $M_{\rm eff}$, which is determined by the expression in the square brackets of Eq. (18). At small opacities, the function $\Phi(\vec{r}\,')$ varies slowly within the beam volume, which allows us to set $\Phi(\vec{r}\,')\simeq\Phi(\vec{r}\,'=0)$. Equation (B1) can thus be reduced to

$$N_{\rm Na^*_{slow}}=\left[\int_{\Omega_{\rm PD}} d^3r'\, n^*_{\rm fast}(\vec{r}\,')\right]\tilde{\Phi}(\vec{r}\,'=0)\,\frac{\overline{N}(r_b=0)}{\Gamma_{\rm nat}},$$

$$\tilde{\Phi}(\vec{r}\,'=0)=\Gamma_{\rm nat}\int_{-\infty}^{\infty} d\nu\int_{\Omega_b} d^3r\, G_\nu(\vec{r},\vec{r}\,'=0)\kappa_\nu(\vec{r})\varepsilon_\nu(\vec{r}). \quad \text{(B4)}$$

The exact representation of function $\tilde{\Phi}(\vec{r}\,'=0)$ coincides with the source function in Eq. (52), $S^*(\vec{r}=0)/n^*_{\rm fast}=\tilde{\Phi}(\vec{r}\,'=0)$, provided that integration over the photodissociation zone $\Omega_{\rm PD}$ in Eq. (36) is replaced by integration over the beam volume Ω_b. This correspondence justifies the replacement of $\Omega_{\rm PD}$ by Ω_b when evaluating the integrals in Eq. (43). It is well seen from the above derivation that the total number of slow excited atoms, $N_{\rm Na^*_{slow}}$, relates to the total number of fast photofragments, $N_{\rm Na^*_{fast}}$, whereby this relation does not depend on the spatial distribution of $n^*_{\rm fast}(\vec{r}\,')$ and the shape of the photodissociation zone $\Omega_{\rm PD}$. Hence it does not depend also on the intensity profile of the photodissociation laser.

APPENDIX C: EFFECT OF HFS ON RADIATION IMPRISONMENT

Under the conditions considered in this study, the HFS of the upper level $3p_{3/2}$ is not resolved, but the lower level $3s_{1/2}$ is split into two spectrally resolved components $F=1$ and $F=2$. Hence the imprisonment of radiation within the ensemble of slow Na($3s_{1/2}$) atoms occurs on two different transitions. This requires a proper modification of the kernel entering the integral term of the imprisonment Eq. (9) and Eq. (14) describing the mean number of scattering events, $\overline{N}_\nu(\vec{r})$. Using the sum rules for the HFS spectra,[30] we can rewrite the kernel G_ν of the imprisonment Eq. (9) as

$$G^{(\rm eff)}_\nu(\vec{r},\vec{r}\,')=\tfrac{3}{8}G^{(1)}_\nu(\vec{r},\vec{r}\,')+\tfrac{5}{8}G^{(2)}_\nu(\vec{r},\vec{r}\,'), \quad \text{(C1)}$$

where $G^{(F)}_\nu$ is given by Eq. (10) in which κ_0 is replaced by $\kappa^{(F)}_0$. The integral in Eq. (9) with kernel $G^{(\rm eff)}_\nu(\vec{r},\vec{r}\,')$ describes the situation when the slow excited Na($3p_{3/2}$) atoms emit photons on two well-resolved hyperfine transitions to the $F=1$ and $F=2$ levels of the ground state with relative probabilities $\overline{g}_F/8$. The radiation diffusion in the beam is therefore described as two independent imprisonment processes with different partial absorption coefficients $\kappa^{(F)}_0$ corresponding to each of the hyperfine transitions.

Using the kernel given by Eq. (C1), the equation describing the mean number of scattering events, $\overline{N}^{(\rm eff)}_\nu(\vec{r})$, under the conditions of resolved HFS of the ground state becomes

$$\overline{N}^{(\rm eff)}_\nu(\vec{r})-\int_{\Omega_b} d^3r'\, G^{(\rm eff)}_\nu(\vec{r},\vec{r}\,')\overline{N}^{(\rm eff)}_\nu(\vec{r}\,')=1. \quad \text{(C2)}$$

The solution of Eq. (C2) can be found using the approach introduced in Secs. III A and IV D. First, the Fokker–Planck approach is used to find $\overline{N}^{(\rm eff)}_\nu$ at large opacities, and the result is then extrapolated into the region of small opacities. The Fokker–Planck method is manifested by Eq. (15) with boundary conditions (16), whereby we keep in mind the asymptotic properties [Eqs. (32) and (33)] of the Fourier transform $V^{(\rm eff)}(p)$ of the kernel $G^{(\rm eff)}_\nu$ given by Eq. (25). Using Eqs. (25) and (26) and the definition of the kernel given by Eq. (10), the function $V^{(\rm eff)}$ for an absorbing medium with non-negligible HFS splitting can be written as

$$V^{(\rm eff)}(\tilde{p})=\frac{5}{8}V\left(\frac{8}{5}\tilde{p}\right)+\frac{3}{8}V\left(\frac{8}{3}\tilde{p}\right),$$

$$\tilde{p}=p/\zeta_\nu=\frac{p}{\kappa_0\exp(-v^2/\Delta v^2_{\rm at})}, \quad \text{(C3)}$$

for all values of its argument. Using Eq. (32), which implies that at large opacities $V(\tilde{p})\simeq\tilde{p}^2/15$, we obtain

$$V^{(\rm eff)}(\tilde{p})|_{\tilde{p}\to 0}\simeq\frac{\tilde{p}^2}{15}\left(\frac{8}{5}+\frac{8}{3}\right)\simeq V\left(\tilde{p}\,\frac{8}{\sqrt{15}}\right),$$

$$\kappa_0\to\kappa^{(\rm eff)}_0=\frac{\sqrt{15}}{8}\kappa_0. \quad \text{(C4)}$$

According to the definition of $\tilde{p}$ in Eq. (C3), the modification of argument of the function V in Eq. (C4) is equivalent to the replacement of the absorption coefficient κ_0 for a medium without HFS by the effective absorption coefficient $\kappa^{(\rm eff)}_0$. Note that in Eq. (C4) the functions $V^{(\rm eff)}(\tilde{p})$ and $V(\tilde{p}8/\sqrt{15})$ are equal to within 4% or less for all values of $\tilde{p}$ of interest. Since the imprisonment equations with HFS are uniquely determined by the function $V^{(\rm eff)}$ [see Eqs. (27) and (31)], it is possible to account for the HFS splitting of the ground state by replacing $\kappa_0 R$ with the effective opacity $\kappa^{(\rm eff)}_0 R=(\sqrt{15}/8)\kappa_0 R$.

[1] E. A. Milne, J. London Math. Soc. **1**, 40 (1926).
[2] T. Holstein, Phys. Rev. **72**, 1212 (1947); **83**, 1159 (1951).
[3] L. M. Biberman, Zh. Eksp. Teor. Fiz. **17**, 416 (1947).
[4] N. N. Bezuglov, A. F. Molisch, A. N. Klyucharev, F. Fuso, and M. Allegrini, Phys. Rev. A **57**, 2612 (1998).

[5] N. N. Bezuglov, A. F. Molisch, A. N. Klyucharev, F. Fuso, and M. Allegrini, Phys. Rev. A **59**, 4340 (1999).
[6] H. A. Post, Phys. Rev. A **33**, 2003 (1986).
[7] A. F. Molisch, B. P. Oehry, W. Schupita, and G. Magerl, J. Phys. B **30**, 1879 (1997).
[8] N. N. Bezuglov and V. N. Gorshkov, Opt. Spektrosk. **56**, 1000 (1984) [Opt. Spectrosc. **56**, 614 (1984)].
[9] N. N. Bezuglov, A. N. Klyucharev, and V. A. Sheverev, J. Phys. B **20**, 2495 (1987).
[10] M. L. Janson and S. M. Papernov, J. Phys. B **15**, 4175 (1982).
[11] H. Hulsman and P. Willems, Chem. Phys. **119**, 377 (1988).
[12] J. Huennekens, R. K. Namiotka, J. Sagle, Z. J. Jabbour, and M. Allegrini, Phys. Rev. A **51**, 4472 (1995).
[13] O. Kaufmann, A. Ekers, K. Bergmann, N. Bezuglov, K. Miculis, M. Auzinsh, and W. Meyer, J. Chem. Phys. **119**, 3174 (2003).
[14] R. I. Asadullina, N. N. Bezuglov, and E. N. Borisov, Opt. Spektrosk. **67**, 360 (1989) [Opt. Spectrosc. **67**, 208 (1989)].
[15] V. V. Ivanov, *Transfer of Radiation in Spectral Lines*, NBS Special Publication No. 385 (U.S. GPO, Washington, D.C., 1973).
[16] L. M. Biberman, V. S. Vorobjev, and I. T. Yakubov, *Kinetics of Nonequilibrium Low-Temperature Plasma* (Plenum, New York, 1987).
[17] A. F. Molisch and B. P. Oehry, *Radiation Trapping in Atomic Vapors* (Oxford University Press, Oxford, 1998).
[18] A. Hishikawa, T. Fujimoto, and P. Erman, Phys. Rev. A **52**, 189 (1995).
[19] D. E. Rees, in *Numerical Radiative Transfer*, edited by W. Kalkofen (Cambridge University Press, Cambridge, England, 1987).
[20] A. G. Mitchell and M. W. Zemanski, *Resonance Radiation and Excited Atoms* (Cambridge University Press, Cambridge, England, 1961).
[21] N. N. Bezuglov, A. N. Klyucharev, A. F. Molisch, M. Allegrini, F. Fuso, and T. Stacewicz, Phys. Rev. E **55**, 3333 (1997).
[22] A. N. Klyucharev and N. N. Bezuglov, *Processes of Excitation and Ionization of Atoms During Light Absorption (Optically Excited Media)* [*Processy vozbuzhdenija i ionizacii atomov pri pogloshenii sveta (opticheski vozbuzhdennye sredy)*] (Leningrad State University Press, Leningrad, 1983).
[23] I. S. Gradstein and I. M. Ryzhik, *Tables of Series, Products and Integrals* (Academic, New York, 1994).
[24] B. Kaulakys and A. Ciziunas, J. Phys. B **20**, 1031 (1987).
[25] N. N. Bezuglov, V. M. Borodin, A. K. Kazanskii, A. N. Klyucharev, A. A. Matveev, and K. V. Orlovskii, Opt. Spektrosk. **91**, 25 (2001) [Opt. Spectrosc. **91**, 19 (2001)].
[26] V. A. Veclenko, Zh. Eksp. Teor. Fiz. **36**, 204 (1959).
[27] N. N. Bezuglov, A. K. Kazansky, F. Fuso, and M. Allegrini, Phys. Rev. A **63**, 042703 (2001).
[28] L. D. Landau and E. M. Lifshitz, *Quantum Mechanics* (Pergamon, New York, 1977).
[29] L. de Broglie, Ph.D. thesis, Musson et Co., Paris, 1924.
[30] H. G. Kuhn, *Atomic Spectra* (Longman, London, 1969).
[31] N. N. Bezuglov, A. F. Molisch, A. Fioreti, C. Gabbanini, F. Fuso, and M. Allegrini (unpublished).